Molecular Cancer Research

SMAD4 suppresses AURKA-induced Metastatic Phenotypes via Degradation of AURKA in a TGF-beta-independent manner

Lina Jia, Hun Seok Lee, Chun Fu Wu, et al.

Mol Cancer Res Published OnlineFirst July 24, 2014.

SMAD4 suppresses AURKA-induced Metastatic Phenotypes via Degradation of AURKA in a TGF-β-independent manner

Lina Jia [1,a], Hun Seok Lee [2,a], Chun Fu Wu [1], Juthika Kundu [4], Sang Gyu Park [5], Ryong Nam Kim [2,6], Li-Hui Wang [1], Özgür Cem Erkin [7], Jong-Sun Choi [6], Seoung Wan Chae [8], Ho Bin Yang [2], Yoon-La Choi [9], Young Kee Shin [2,3,6*]

[1] Department of Pharmacology, School of Life Science and Biopharmaceutics, Shenyang Pharmaceutical University, Shenyang, China
[2] Research Institute of Pharmaceutical Science, Department of Pharmacy, College of Pharmacy, Seoul National University, Seoul, Korea
[3] The Center for Anti-cancer Companion Diagnostics, Institutes of Entrepreneurial BioConvergence, Seoul National University, Seoul, Korea
[4] College of Pharmacy, Keimyung University, Deagu, Korea
[5] Laboratory for Tracing of Gene Function, Department of Biomedical Science, CHA Stem Cell Institute, CHA University, Gyeonggido, Korea
[6] Tumor Microenvironment Global Core Research Center, Seoul National University, Seoul, Korea.
[7] Department of Bioengineering, Faculty of Engineering, Adana Science and Technology, Adana, Turkey
[8] Department of Pathology, Kangbuk Samsung Hospital, Sungkyunkwan University School of Medicine, Seoul, Korea
[9] Department of Pathology, Samsung Medical Center, Sungkyunkwan University School of Medicine, Seoul, Korea

[*] Corresponding author address: Laboratory of Molecular Pathology, Department of Pharmacy, College of Pharmacy, Seoul National University, 599 Gwanak-ro, Gwanak-gu, Seoul 151-742, Korea. Tel.: +82-2-880-9126; Fax: +82-2-883-9126.
E-mail addresses: ykeeshin@snu.ac.kr
[a] These authors contributed equally to this work.

Running Title: SMAD4 suppresses AURKA in a TGF-β-independent manner

Keywords: SMAD4; Tumor suppression; AURKA; WNT/β-catenin signaling

Abstract

SMAD4 has been suggested to inhibit the activity of WNT/β-catenin signaling pathway in cancer. However, the mechanism by which SMAD4 antagonizes WNT/β-catenin signaling in cancer remains largely unknown. Aurora A kinase (AURKA), which is frequently overexpressed in cancer, increases the transcriptional activity of β-catenin/T cell factor (TCF) complex by stabilizing β-catenin through the inhibition of GSK-3β. Here, SMAD4 modulated AURKA in a TGF-β-independent manner. Overexpression of SMAD4 significantly suppressed AURKA function including colony formation, migration, and invasion of cell lines. In addition, SMAD4 bound to AURKA, induced degradation of AURKA by the proteasome. A luciferase activity assay revealed that the transcriptional activity of the β-catenin/TCF complex was elevated by AURKA, but decreased by SMAD4 overexpression. Moreover, target gene analysis showed that SMAD4 abrogated the AURKA-mediated increase of β-catenin target genes. However, this inhibitory effect of SMAD4 was abolished by overexpression of AURKA or silencing of AURKA in SMAD4-overexpressed cells. Meanwhile, the SMAD4-mediated repression of AURKA and β-catenin was independent of TGF-β signaling because blockage of TGF-βR1 or restoration of TGF-β signaling did not prevent suppression of AURKA and β-catenin signaling by SMAD4. These results indicate that the tumor-suppressive function of SMAD4 is mediated by down-regulation of β-catenin transcriptional activity via AURKA degradation in a TGF-β-independent manner.

Implications: SMAD4 interacts with AURKA and antagonizes its tumor promoting potential, thus demonstrating a novel mechanism of tumor suppression.

Introduction

SMAD4, alternatively known as DPC4 (deleted in pancreatic carcinoma), is a tumor suppressor protein (1). As the only known common mediator (Co)-SMAD in mammals, SMAD4 is thought to be involved in anti-proliferative signaling induced by all members of the transforming growth factor (TGF)-β superfamily (2). Although the tumor suppression function of SMAD4 has primarily been attributed to its ability to mediate TGF-β growth inhibitory responses, several studies have shown that the anti-tumor function of SMAD4 is not solely dependent on the restoration of TGF-β anti-proliferative responses (3, 4). Thus, identifying the pathways critical for the tumor suppressor function of SMAD4 remains to be determined.

One of the mechanisms by which SMAD4 suppresses tumor progression is by modulating the WNT/β-catenin signaling pathway (5, 6). Aberrant activation of β-catenin as a key effector of the WNT signaling cascade could lead to cancer development (7-10). Recent evidence has revealed that the restoration of SMAD4 in SMAD4-deficient SW480 colon carcinoma cells resulted in suppression of WNT/β-catenin signaling activity and migration capacity in human colon carcinoma cells (11). In HEK293T cells, inhibition of bone morphogenetic protein (BMP) signaling or loss of SMAD4 can similarly augment β-catenin levels through a transcriptional mechanism, resulting in stimulation of WNT signaling (6). However, the molecular mechanism by which SMAD4 negatively regulates β-catenin signaling has not been identified.

Aurora A kinase (AURKA), a centrosomal serine/threonine protein kinase, is overexpressed and localized to centrosomes during interphase and to spindle poles during mitosis because of constitutive phosphorylation (12) through activation of

oncogenic RAS (13) and the MAPK pathway (14). AURKA is commonly amplified in a wide range of human cancers including ovarian, breast, colorectal, pancreatic, bladder, and gastric cancers, and the gene copy number, mRNA level, and protein level are also increased in those cancers (15-19).

The role of AURKA in human carcinogenesis might be different among cancer types or cancer stages. Overexpression of AURKA contributes to carcinogenesis by promoting oncogenic transformation (13), and speeding up the rate of metastasis (20, 21); however, inhibition of AURKA expression results in marked growth suppression *in vitro* and abolishes tumorigenicity *in vivo* (22-25). AURKA directly phosphorylates glycogen synthase kinase (GSK)-3β and activates β-catenin in response to tumorigenic stimuli (26). Moreover, AURKA exerts its cell survival signal through activation of the AKT pathway (27), which inactivates target GSK-3β via phosphorylation to promote β-catenin stabilization (28).

While SMAD4 has been reported to inhibit RAS-dependent extracellular signal-regulated kinase (ERK) activity in RAS-transformed keratinocytes (29), overexpression of AURKA potentiates RAS-mediated oncogenic transformation (13). Thus, we hypothesized that the tumor suppressor function of SMAD4 is inversely correlated with the oncogenic role of AURKA. Since β-catenin-mediated signaling is enhanced by activation of AURKA (26) and diminished by overexpression of SMAD4 (6, 11), we examined the possibility of cross-talk between SMAD4 and AURKA in the regulation of WNT/β-catenin signaling. We found that SMAD4 not only suppresses the expression levels of AURKA, but also antagonizes AURKA-mediated tumorigenicity through interactions between SMAD4 and AURKA. Therefore, AURKA is required for SMAD4-mediated suppression of WNT/β-catenin signaling in cancer, thereby becoming

a novel interaction partner for the tumor suppressor function of SMAD4.

Materials and methods

Cell culture, transient transfection, and chemical treatment

The human gastric cancer cell line AGS, colon cancer cell line SW480, and cervical cancer cell line HeLa were obtained from the Korean Cell Line Bank (KCLB, Seoul, Korea). The mouse embryonic fibroblasts NIH3T3 was purchased from American Type Culture Collection (ATCC, Manassas, VA). NIH3T3 cells were maintained in Dulbecco's modified Eagle's medium and AGS, SW480, and HeLa cells were maintained in RPMI 1640 supplemented with 10% fetal bovine serum and 1× penicillin/streptomycin at 37˚C in 5% CO_2 atmosphere. Cells were routinely checked for mycoplasma contamination. For transient transfections, cultured cell lines have been carried out using Genefectine^{TM} Reagent (Genetrone Biotech, Gyeonggido, Korea) according to the manufacturer's recommended protocol. Typically, equal numbers of cells were seeded to 100-mm dishes 24 h prior to the transfection and transfected with different plasmids at a total concentration of 5 μg. After transfection of 36 h, cells were treated with MG132 (Merck KGaA, Darmstadt, Germany) or dimethylsulfoxide (Sigma-Aldrich Chemical Co., St. Louis, MO) as a control for 12 h prior to harvesting. TGF-β1 (Komabiotech, Seoul, Korea) or A83-01 (Tocris Bioscience, Bristol, UK) treatment was performed after transfection 20 h for 2 h prior to harvesting.

Western blotting analysis

Cells were routinely lysed at 24 h post-transfection in RIPA buffer [150 mM NaCl, 10 mM Tris (pH 7.2), 0.1% sodium dodecyl sulphate (SDS), 1% Triton X-100, 1% sodium deoxycholate and 5 mM ethylenediaminetetraacetic acid (EDTA)] enriched with a

complete protease inhibitor cocktail tablet and phosphatase inhibitor cocktail tablet (Roche Diagnostics, Basel, Switzerland), and then incubated on ice for 20 min with regular vortexing before centrifuging at 14,000 rpm, 4°C, for 15 min. Protein concentration was determined using a bichinconinic acid (BCA) protein assay kit (Pierce Biotechnology, Rockford, IL). The protein samples were boiled with SDS sample buffer for 10 min for complete denaturation and were resolved on 7-10% SDS-polyacrylamide gels. After electrophoresis, proteins were transferred onto polyvinyl difluoride (PVDF) membrane, which was blocked with 5% nonfat dry milk in TBS-T and incubated with primary antibody at the appropriate final concentration followed by hybridization with horseradish peroxidase (HRP)-conjugated secondary antibodies for visualization. The primary antibodies used were as follows: SMAD4, AURKA, MYC, ACTB, β-catenin, HA, and uPAR were purchased from Santa Cruz Biotechnology (St. Louis, CA); AKT1, pAKT (Ser 473), GSK-3β, pGSK-3β (Ser 9), CCND1, SMAD2/3, and pSMAD2 (Ser 465/467)/SMAD3 (Ser423/425) were purchased from Cell Signaling (Danvers, MA).

Establishment of overexpressing AURKA-NIH3T3 cells

NIH3T3 cells were seeded into 6-well cell culture plates to provide a final density of 70-80% confluence 24 h before transfection. Cells were transfected using Genefectine™ Reagent (Genetrone Biotech) according to the manufacturer's recommended protocol and selected in complete medium containing 1 mg/mL G418 sulfate (Life Technologies) at 48 h after transfection. G418-resistant cell clones were isolated for 2 weeks and screened for expression of *FLAG*-AURKA by western blotting analysis.

Anchorage-independent cell transformation assay

One clone of NIH3T3 cells that overexpressed *FLAG*-AURKA was used. NIH3T3 cells that were stably transfected with 3×*FLAG* vector were used as a control. The overexpressing AURKA NIH3T3 cells were transiently transfected with 6*Myc-SMAD4* as described before. After 24 h post transfection, cells were trypsinized and suspended in 1 mL 0.33% basal medium Eagle's (BME) agar and poured onto 3 mL of 0.5% BME agar containing 10% FBS. Four weeks later, cell colonies were counted using a microscope (Nikon).

Cell migration and invasion assay

AGS, SW480, and HeLa cells were transiently transfected with the indicated DNA or siRNA as described before. Cells were prepared 48 h post-transfection and were subjected to Chemicon QCM™ Cell Migration Assay and QCM™ Fluorimetric Cell Invasion Assay systems (Merck Millipore, Billerica, MA). After incubation for 48 h at 37°C, cell number was detected with a GENios Pro microplate reader (Tecan Trading AG) using 485/535 nm filter set. All migration and invasion assays were performed in at least three independent experiments. Values are expressed as percentages compared to controls.

Synchronization and cell cycle analysis

Cell synchronization at the G1/S phase was performed using a double-thymidine block (DTB) (30). HeLa cells were transfected with empty vector, SMAD4, AURKA, or a combination for 36 h and treated with MLN8237 (100 nM) or dimethyl sulfoxide

(DMSO). Thymidine (Sigma-Aldrich Chemical Co.) was added to the complete culture media at a final concentration of 2 mM for 12 h. Following two times washing with serum free media, the cells were released from the thymidine block by culture in complete culture media. After 12 h of incubation, the second thymidine block was initiated and completed after 12 h. The cells were released from the block by washing in warm phosphate-buffered saline (PBS) and replacing with complete culture media for 8 h. The cells fixed in 70% ethanol washed with PBS and then stained with FACS solution [50 μg/mL propidium iodide and 100 μg/mL RNase A in PBS] for 30 min at RT. Cell cycle stages were monitored by flow cytometry using FACSCalibur (BD Biosciences, San Jose, CA).

Co-immunoprecipitation (IP) assay

HeLa cells were lysed in IP buffer [150 mM NaCl, 50 mM Tris (pH 7.4), 0.5% sodium deoxycholate, 1% Triton X-100] enriched with a complete protease inhibitor cocktail tablet and phosphatase inhibitor cocktail tablet. Cells lysate was rotated with anti-AURKA antibody or normal goat IgG (4 μg) for overnight at 4°C and soluble supernatant fractions were obtained by centrifugation at 4,000 rpm for 3 min at 4°C. Soluble fractions were combined with 50 μL γprotein G agarose beads (Life Technologies) followed by rotation for 2.5 h at 4°C. Agarose bead-complexes were sequentially washed 3 times with PBS buffer including 1% Triton X-100. Bound proteins were eluted by boiling with SDS sample buffer for 10 min and subjected to sodium dodecyl sulfate-polyacrylamide gel electrophoresis followed by Western blotting.

Ubiquitination assay

HeLa cells transiently transfected with *HA-tagged Ub* (1 μg), *FLAG-tagged AURKA* (2 μg) or *FLAG-tagged AURKA mutants* (K5R, K117R, K389R, and K401R) with or without 6*Myc-tagged SMAD4* (6 μg), were harvested after 36 h post-transfection in an IP buffer, and IP was conducted with anti-*FLAG*-M2 antibody (1 μg). Immunoprecipitated samples were washed stringently 3 times in PBS buffer supplemented with 1% Triton X-100, boiled for 10 min and eluted proteins were subjected to western blot analysis with anti-*FLAG*-M2 (Sigma-Aldrich Chemical Co.), anti-*HA*, or anti-*Myc* (Santa Cruz Biotechnology) antibodies to detect AURKA-Ub conjugates.

***SMAD4* or *AURKA* small interfering RNA (siRNA)**

AURKA siRNA and non-targeting control siRNA were purchased from Genolution Pharmaceuticals Inc. (Seoul, Korea). *AURKA* siRNA: sense, GAA UCA GCU AGC AAA CAG UUU; antisense, ACU GUU UGC UAG CUG AUU CUU. The on-target plus smart pool siRNA to human *SMAD4* (L-003902–00) and a scrambled siRNA duplex were purchased from Thermo Fisher Scientific (Waltham, MA). *SMAD4* siRNA: sense, CAC CAG GAA UUG AUC UCU CAG GAU U; antisense, AAU CCU GAG AGA UCA AUU CCU GGU G. Transfection was performed using Oligofectamine™ Reagent (Life Technologies, Grand Island, NY) according to the manufacturer's instructions. Silencing of SMAD4 was performed with *SMAD4* siRNA (5 or 10 nM) transfection for 24 h. Silencing of AURKA was performed with 10 nM of *AURKA* siRNA transfection for 72 h.

The Bimolecular fluorescence complementation (BiFC) analysis

BiFC constructs using fragments derived from newly engineered fluorescent protein-Venus, was kindly provided by Professor Chang-Deng Hu (Department of Medicinal Chemistry and Molecular Pharmacology and Purdue Cancer Center, Purdue University, West Lafayette, IN). cDNAs encoding AURKA, AURKA-C (residues 102-404), and AURKA-N (residues 1-129) were amplified by PCR from a human cDNA library and sub-cloned into a p*FLAG*-CMV vector to make BiFC fusion constructs with VN173. cDNAs encoding SMAD4, SMAD4-MH1 (residues 1-145), SMAD4-MH2 (residues 321-553), and SMAD4-linker (residues 140-325) were amplified by PCR from a human cDNA library and sub-cloned into a p*HA*-CMV vector to make BiFC fusion constructs with VC155. BiFC analysis was performed essentially as previously described. The detectable fluorescence was the indicator of protein-protein interaction after co-transfection of VC155 and VN173 plasmids. Fluorescence images were captured using a charge-coupled device (CCD) camera mounted on a TE2000-U inverted fluorescence microscope (Nikon, Melville, NY) with JP4 filters (Chroma, Rockingham, VT).

Competition assay

HeLa cells transiently transfected with *FLAG-VN173-tagged AURKA* (0.5 μg), *HA-VC155-tagged SMAD4* (0.5 μg) with or without 3×*FLAG-tagged AURKA* as indicated concentrations. Cells were subjected to BiFC analysis after 18 h post-transfection. The detectable fluorescence signals were counted using a microscope (Nikon).

The proximity ligation (PLA) assay

The PLA experiments on cultured HeLa cells were performed according as

manufacturer's protocol (O-LINK Bioscience, Uppsala, Sweden). Fixed cells on 4 well-cell culture slide (SPL Life Sciences Co., Gyeonggido, Korea) using 4% paraformaldehyde were blocked with 5% non-fat milk for 60 min and then incubated with the primary antibody of AURKA together SMAD4 antibody at 1:100 dilution for overnight at 4˚C. Then, cells on slide were washed two times with TBS-T (Tris-buffered saline with 0.1% Tween-20) for 5 min, incubated with the PLA probe solutions for 60 min at 37˚C, washed two times with TBS-T for 5 min, and incubated with the ligase solution for 30 min at 37˚C for ligation. After the ligation solution was removed, samples were washed two times with TBS-T for 2 min and incubated with the polymerase solution for 100 min at 37˚C for amplification. Finally, the samples were washed with SSC buffers (made up according to the manufacturer's recipe) and ethanol and then mounted. The slides were analyzed for digital micrographs using a LSM 700 ZEISS laser scanning confocal microscope (Carl Zeiss, Jena, Germany).

Immunofluorescence

For double immunofluorescent staining, fixed cells on 8well-cell culture slide (SPL) using 4% paraformaldehyde were blocked with 5% non-fat milk for 60 min and then incubated with the primary antibody against AURKA together SMAD4 antibody at 1:100 dilution for overnight at 4˚C. The secondary antibodies were alexa fluor 488-conjugated goat anti-mouse IgG (1:100, Molecular Probes, Carlsbad, CA) and alexa fluor 546-conjugated goat anti-rabbit IgG (1:100, Molecular Probes) and were incubated for 1 h at RT. Finally, the samples were washed three times with PBS with 1% Triton x-100 and then mounted. The slides were analyzed for digital micrographs using a LSM 700 ZEISS laser scanning confocal microscope. The nucleus of HeLa cells for

immunofluorescence was stained with Hoechst 33342 (Life Technologies).

Luciferase reporter gene assay

Cells were seeded into 12-well plates at a density of 1×10^5 cells/well and grown in growth media for 24 h prior to transfection. pTOPFlash and pFOPFlash reporter plasmids were kindly provided by Professor Sung-Hee Baek (College of Natural Sciences, Seoul National University, Korea). pRL-TK (Promega, Madison, WI) was used as a normalization control. After 24 h of transfection, the luciferase activity was measured using the Dual-Luciferase® Reporter Assay System according to the manufacturer's instructions (Promega), followed by luminescence measurement in a GENios Pro microplate reader (Tecan Trading AG, Männedorf, Switzerland). The activated firefly luciferase activity was normalized to the internal control activity by pRL-TK.

Quantitative real-time polymerase chain reaction (qRT-PCR) analysis

Total RNA was extracted from transfected cells using Hybrid-RTM total RNA Kit (GeneAll Biotechnology, Seoul, Korea). Approximately 2 μg DNase I-treated RNA samples were reverse transcribed to cDNAs using the Superscript™ II First-Strand Synthesis System (Life Technologies). Following cDNA synthesis, qRT-PCR was performed as described in a dual system LightCycler (Roche Diagnostics) and the expression levels of target genes relative to HPRT were determined by a SYBR Green-based comparative CT method (relative fold change = $2^{-\Delta\Delta CT}$). Primers used are as follows: *Cyclin D1*: sense, GAA GAT CGT CGC CAC CTG, antisense, GAC CTC CTC CTC GCA CTT CT; *c-MYC*: sense, CAC CAG CAG CGA CTC TGA, antisense, GAT

CCA GAC TCT GAC CTT TTG C; *uPAR*: sense, ACA CCA CCA AAT GCA ACG A, antisense, CCC CTT GCA GCT GTA ACA C; *HPRT*: sense, CTC AAC TTT AAC TGG AAA GAA TGT C, antisense, TCC TTT TCA CCA GCA AGC T. All PCR primers were purchased from Cosmo Genetech (Seoul, Korea).

Patient tissues and immunohistochemical analysis

Using 241 gastric tissue samples from Samsung Medical Center (Seoul, Korea), a tissue microarray (TMA) with 3-mm diameter tissue columns was constructed. SMAD4 or AURKA immunostaining were performed using mouse anti-SMAD4 or goat anti-AURKA antibodies, respectably (1:50 dilution, Santa Cruz Biotechnology), as previously reported (31). The staining intensity and proportion of positively stained tumor cells were evaluated, and an immunoreactive score (IS) for each sample was generated, as previously described (32).

Copy number alteration, RNA expression and mutation analyses of *AURKA*, *SMAD4* and β-catenin gene (*CTNNB1*) using The Cancer Genome Atlas (TCGA) database

Using copy number alteration, RNA-Seq and mutation data of 17,584 human samples of diverse cancer types in TCGA database, amplification, deletion and mutation statuses of *AURKA*, *SMAD4* and *CTNNB1* were shown in **Supplementary Figure 2**.

Statistical analysis

Data are presented as the means ± SD of triplicate samples from at least three independent experiments (n=3). Comparisons were made using Student's *t*-test was

considered significant when $P < 0.05$.

Results

SMAD4 inversely regulates AURKA function in cancer cells

SMAD4 inhibits the progression of colon (11) and gastrointestinal (6) cancer by suppressing the activity of β-catenin; however, AURKA promotes tumor progression by activating the β-catenin pathway (26). To identify a functional link among SMAD4, AURKA and β-catenin in cancer, we examined the expression of these proteins in a variety of cancer cells as well as in normal cells. We detected β-catenin protein expression in cells (AGS, MKN28, and SW480) in which the expression ratio of AURKA to SMAD4 was greater than one. In contrast, β-catenin protein expression was minimal or undetectable in the cells examined (NIH3T3, HaCaT, MKN1, SNU484, SNU668, SiHa, HeLa, A549, HepG2, MDA-MB231, and SKOV3) where the expression ratio of AURKA to SMAD4 was less than one (**Fig. 1A**). An inverse correlation was observed between the expression of SMAD4 and that of AURKA, and their relationship with β-catenin expression in cancer cells prompted us to first examine whether SMAD4 can modulate AURKA function in cancer. We stably transfected NIH3T3 cells with *FLAG-AURKA* and performed a 12-*O*-tetradecanoylphorbol-13-acetate (TPA)-induced colony formation assay following co-transfection with either a control vector or with 6*Myc-SMAD4*. Overexpression of AURKA in all 4 stable clones was confirmed based on *FLAG* expression (data not shown). Stable clones of NIH3T3 cells overexpressing AURKA were transiently transfected with 6*Myc-SMAD4* or empty vector and subjected to colony formation assay. Since AURKA has only weak oncogenic activity and lacks the capacity to transform NIH3T3 cells by itself alone (18), the colony formation assay was performed by treating cells with a proto-type tumor promoter TPA (20 μg/mL). Treatment with TPA significantly increased the colony numbers of AURKA-

overexpressing NIH3T3 cells compared to cells transfected with the empty vector, while co-transfection of AURKA-overexpressing NIH3T3 cells with 6*Myc-SMAD4* resulted in a substantial decrease in the number of transformed colonies (**Fig. 1B**).

To further examine the inhibitory effect of SMAD4 on AURKA function, we performed a migration and invasion assay using AGS, SW480, and HeLa cells. As expected, overexpression of SMAD4 suppressed the migration and invasion of AGS, SW480, and HeLa cells compared to control cells (**Fig. 1C and D**). Compared to empty vector-transfected cells, transfection of AGS, SW480, and HeLa cells with *AURKA* significantly increased migration and invasion, which then could be markedly inhibited by co-transfection of these cells with 6*Myc-SMAD4* (**Fig. 1C and D**). These findings suggest that SMAD4 antagonizes the oncogenic activity of AURKA and the suppressive effects mediated by SMAD4 were partly reversed by *AURKA* transfection.

In order to rule out the possibility that inhibitory effects of SMAD4 on AURKA function are consequences of cell cycle abnormalities because SMAD4 overexpression induces a significant increase of G1 populations (33) and ectopic overexpression of AURKA in cells accelerates G2/M progression (34), cell cycle analysis with double thymidine treatment was performed. Similarly, overexpression of SMAD4 slightly increased in G1 phase and AURKA overexpression reversed the ratio of G1 to G2/M phase compared to empty vector-transfected cells (**Fig. 1E**). However, expression of SMAD4 with AURKA transfection could not significantly alter the cell cycle progression compared to control cells. The selective inhibitor for AURKA, MLN8237, induces G2/M arrest (35). This MLN8237-induced G2/M arrest was changed to G1 arrest with transfection of SMAD4, whereas most cells transfected with AURKA or a combination of SMAD4 and AURKA remained in G2/M phase, indicating that

regulation of AURKA function by SMAD4 is not a consequence of a cell cycle arrest (**Fig. 1F**).

SMAD4 inhibits expression of AURKA via proteasomal degradation

Because co-transfection of AURKA-overexpressing NIH3T3 cells with 6*Myc-SMAD4* reduced AURKA expression, we examined whether SMAD4 could diminish AURKA expression in AGS, SW480, HeLa, and HaCaT cells. As shown in **Fig. 2A**, expression of endogenous AURKA was dramatically decreased by overexpression of SMAD4. In contrast, siRNA-mediated silencing of SMAD4 increased AURKA expression in AGS and HeLa cells in a dose-dependent manner (**Fig. 2B**). Although SMAD4 reduced AURKA protein expression, it did not affect AURKA mRNA expression of (data not shown). We therefore investigated whether SMAD4 could enhance proteasomal degradation of AURKA in cancer cells. HeLa cells transfected with 6*Myc-SMAD4* were treated with the proteasome inhibitor MG132 (10 μM) or DMSO as a control for 12 h. In HeLa cells, the inhibitory effect of SMAD4 on AURKA and β-catenin expression which is a downstream target of AURKA was abrogated by treatment with MG132 (**Fig. 2C**). Because the proteasome is a subcellular organelle that degrades ubiquitin (Ub)-tagged protein, we determined whether SMAD4 could promote Ub-dependent degradation of AURKA. An ubiquitination assay involving immunoprecipitation (IP) showed that SMAD4 promoted the ubiquitination of wild-type AURKA, but not of K389R mutant AURKA, suggesting that the K389 residue of AURKA is critical for ubiquitination-dependent degradation of AURKA by SMAD4 (**Fig. 2D**).

SMAD4 interacts with AURKA

To further characterize SMAD4-mediated regulation of AURKA, we examined whether SMAD4 could interact with AURKA. IP of AURKA from HeLa cells using western blotting revealed that endogenous SMAD4 co-immunoprecipitated with endogenous AURKA (**Fig. 3A**). The interaction between SMAD4 and AURKA was confirmed using a bimolecular fluorescence complementation (BiFC) assay, which has been widely used to examine protein-protein interactions in living cells (36, 37). In this study, we fused sequences encoding SMAD4 to the *pHA-CMV* expression vector containing venus residues 155–238 (VC155). Sequences encoding AURKA were fused to the *pFLAG-CMV* expression vector containing venus residues 1–173 (VN173). As shown in **Figure 3B**, after co-transfection of the plasmid encoding SMAD4 and AURKA into HeLa cells, a fluorescence signal was detected nearly exclusively in the cytoplasm, suggesting that SMAD4 and AURKA interact in the cytoplasm. Expression of either AURKA or SMAD4 alone did not produce a detectable fluorescent signals in the BiFC assay (**Supplementary Fig. 1A**, upper panels). As reported previously, R-SMADs (SMAD2 and SMAD3) form heteromeric complexes with SMAD4 through the MH2 domain (38). Thus, the MH1 domain of SMAD2 was used as a negative control (SMAD2-MH1-VN173, residues 9–176), whereas the MH2 domain was used as a positive control (SMAD2-MH2-VN173, residues 274–468) to determine the specificity of BiFC analysis. A fluorescence signal was detected after co-transfection of HeLa cells with plasmids encoding SMAD2-MH2 and SMAD4, but not after transfection with SMAD2-MH1 and SMAD4 (**Fig. 3B**, bottom panels). No fluorescence was observed when VN173 or VC155 fragment were expressed alone (**Supplementary Fig. 1A**, bottom panels). To identify the domain responsible for their interaction, we transfected different combinations of truncated AURKA mutants encompassing the N-terminus (residues

1–129) and C-terminus (residues 101–404), and truncated SMAD4 mutants encompassing the MH1 domain (residues 1–145), linker domain (residues 140–325), and MH2 domain (residues 321–553) into HeLa cells. Of the five aforementioned combinations, three (AURKA:SMAD4-MH1, AURKA:SMAD4-MH2, and SMAD4:AURKA-N-terminus) produced very low signals, while the other two (AURKA:SMAD4-linker and SMAD4:AURKA-C) showed strong fluorescent signals (**Fig. 3B**, top and middle panels). These results indicate that the linker domain of SMAD4 interacts with the C-terminus of AURKA.

To determine the specificity between SMAD4 and AURKA, we examined whether the 3×*FLAG*-AURKA could inhibit the interaction between VC-SMAD4 and VN-AURKA. 3×*FLAG*-AURKA inhibited the interaction between VC-SMAD4 and VN-AURKA in a dose-dependent manner (**Fig. 3C**). This result confirms that fluorescence complementation is mediated by a specific interaction between VC-SMAD4 and VN-AURKA. We further confirmed the endogenous interaction between SMAD4 and AURKA using an *in situ* proximity ligation assay (**Fig. 3D**). Interacting proteins can be detected using two different primary antibodies that are captured against probe-conjugated secondary antibodies. The probes are amplified and then fluorescence is visualized. This assay can be used to detect endogenous protein-protein interactions as well as identify cellular localization. As shown in **Fig. 3E**, we observed nucleic-cytoplasmic expression of SMAD4 and cytoplasmic localization of overexpressed AURKA by using immunofluorescence staining. Similar observations were made in previous studies (39, 40). As shown in the PLA results the interaction of SMAD4 and AURKA was localized to the cytosol, further supporting the findings obtained using HeLa cells (**Fig. 3A and B**). To identify the domain responsible for the interaction

between AURKA and SMAD4, we performed a co-IP experiment using a variety of deletion mutants. Consistent with the results of the BiFC assay, the linker domain of SMAD4 was found to interact with the C-terminus of AURKA (**Fig. 3F, G, and H**). Moreover, both AURKA and β-catenin expressions were decreased to a similar extent by the expression of full-length SMAD4 or only its linker domain, strongly suggesting that the SMAD4 linker domain could play a critical role in its interaction with AURKA, to reduce β-catenin levels (**Fig. 3I**).

SMAD4-mediated downregulation of AURKA inhibited β-catenin signaling

The overexpression of SMAD4 is known to inhibit β-catenin signaling (6, 11), which is amplified by AURKA (26). Because overexpression of SMAD4 downregulated the expression of AURKA, we examined whether inhibition of β-catenin signaling by SMAD4 occurs as a consequence of SMAD4-mediated suppression of AURKA. As expected, overexpression of SMAD4 decreased AKT and GSK-3β phosphorylation, reduced β-catenin expression, and subsequently diminished β-catenin target gene expression, such as *cyclin D1* (*CCND1*) and *urokinase plasminogen activator surface receptor* (*PLAUR*), in AGS and SW480 cells (**Fig. 4A**). Several reports have indicated that the oncogenic functions of β-catenin are mediated by its interaction with members of the TCF/LEF family of transcription factors in the nucleus (41). We performed a pTOPFlash/pFOPFlash luciferase assay to measure the transcriptional activity of the β-catenin/TCF complex. The transcriptional activity of β-catenin was reduced after *SMAD4* transfection (**Fig. 4B**), resulting in decreased mRNA levels of β-catenin target genes, such as *CCND1*, *MYC*, and *PLAUR* (**Fig. 4C**). Overexpression of AURKA in the same cells induced AKT and GSK-3β phosphorylation and β-catenin expression,

leading to increased expression of CCND1 and PLAUR, which was abrogated by co-transfection with *SMAD4* (**Fig. 4A**). In addition, co-transfection with *SMAD4* attenuated the AURKA-mediated increase in β-catenin transcriptional activity (**Fig. 4B**), leading to reduced mRNA levels of β-catenin target genes, including *CCND1*, *MYC*, and *PLAUR* (**Fig. 4C**).

SMAD4 suppressed the β-catenin pathway by targeting AURKA

To address whether the tumor suppression by SMAD4 is directly associated with AURKA, we examined the protein level and transcriptional activity of β-catenin in AGS and SW480 cells co-transfected with *SMAD4* and *AURKA* siRNA. Western blot analysis showed that the protein levels of pAKT, pGSK-3β, and β-catenin were dramatically reduced by overexpression of SMAD4 or silencing of AURKA, but remained unchanged after *SMAD4* transfection in cells in which AURKA had been silenced (**Fig. 5A**). The luciferase activity assay using pTOPFlash/pFOPFlash luciferase vectors in AGS and SW480 cells revealed that the transcriptional activity of β-catenin was inhibited by either SMAD4 overexpression or by AURKA silencing (**Fig. 5B**). These findings were further supported by the reduced expression of β-catenin target genes such as *MYC*, *CCND1*, and *PLAUR* upon transfection of cells with either *SMAD4* or *AURKA* siRNA (**Fig. 5C**). However, *SMAD4* co-transfection with *AURKA* siRNA did not result in synergistic inhibition as compared to transfection with *SMAD4* or *AURKA* siRNA alone. Consistent with these observations, *SMAD4* co-transfection with *AURKA* siRNA did not result in synergistic inhibition of migration and invasion (**Supplementary Fig. 1B and C**). Taken together, our data suggest that SMAD4 mediates the regulation of β-catenin activity by modulating AURKA.

SMAD4-mediated repression of AURKA and β-catenin is independent of TGF-β signaling

To verify whether the downregulation of AURKA and subsequent inactivation of β-catenin by overexpression of SMAD4 in AGS and SW480 cells is dependent on TGF-β signaling, we treated 6*Myc*-SMAD4-overexpressing AGS cells, which express sufficient levels of functional TGF-β receptors (42), with TGF-β1 in the presence or absence of A83-01, a TGF-β receptor 1 (TGF-βR1) inhibitor (43). Phosphorylation of SMAD2/SMAD3 in response to TGF-β1 treatment was observed in cells transfected with SMAD4, but not in cells treated with A83-01 **(Fig. 6A, left panel)**. However, blockage of TGF-βR1 by A83-01 failed to abrogate SMAD4-mediated downregulation of AURKA expression and inhibition of phosphorylation of both AKT and GSK-3β, and diminished the expression of β-catenin and its target genes *PLAUR* and *CCND1* in SMAD4-overexpressing AGS cells **(Fig. 6B, left panel)**. In contrast, SW480 cells express low levels of TGF-β receptor 2 (TGF-βR2) and are not responsive to TGF-β signaling (44). Our study revealed that SMAD4 transfection was not sufficient for transducing TGF-β-mediated SMAD2/SMAD3 phosphorylation unless the cells were co-transfected with TGF-βR2 **(Fig. 6A, right panel)**. Despite the restoration of TGF-β signaling by co-transfecting cells with a construct containing TGF-βR2 along with 6*Myc*-SMAD4, SMAD4-mediated repression of AURKA and β-catenin signaling remained unchanged **(Fig. 6B, right panel)**. These findings suggest that the inhibitory effect of SMAD4 on AURKA expression and β-catenin signaling in AGS and SW480 cells is independent of TGF-β stimulation.

Validation of SMAD4 and AURKA expression in human cancer samples in the cancer genome atlas (TCGA) database

To satisfactorily address our result in human clinical samples, we performed a TMA-based immunohistochemistry to detect SMAD4 and AURKA protein expression in 228 human clinical stomach carcinoma, 4 dysplasia, and 9 normal samples. As shown in **Figures 7A**, SMAD4 expression was the highest in dysplasia cells and markedly lower in carcinomas, while AURKA was expressed at a high level in carcinomas. These results strongly support our basic model in which high AURKA levels in conjunction with low SMAD4 levels could lead to oncogenic activation of β-catenin signaling and progression to the final stage of carcinogenesis. This phenomenon is more apparent in the cytosols than in the nuclei of carcinoma cells, consistent with the finding that AURKA-mediated GSK-3β phosphorylation in the cytosol could induce β-catenin translocation into the nucleus. As shown in **Figure 7B, C, and D**, *AURKA* gene showed high amplification in genome level, in contrast to *SMAD4* gene showing frequent deletion in genome level. In addition, we validated that AURKA was highly overexpressed due to amplification and SMAD4 expression was markedly downregulated due to deletion in 219 gastric carcinoma. These data corroborate the findings reported in this study.

Discussion

SMAD4, as co-SMAD, plays a central role in signaling pathways induced by all members of the TGF-β superfamily. Because SMAD4 mediates TGF-β growth inhibitory responses, previous studies examining the tumor-suppressive functions of SMAD4 have been conducted in the context of TGF-β signaling. However, reactivation of SMAD4 was not sufficient for restoring a TGF-β growth inhibitory response in SW480 cells (3, 4), suggesting that the role of SMAD4 in tumor suppression and understanding its underlying molecular mechanisms require additional investigation. According to previous studies, SMAD4 elicits its antitumor effects by blocking β-catenin signaling (6, 11) which is amplified by AURKA (26). Therefore, we examined whether the downregulation of β-catenin signaling by SMAD4 is mechanistically associated with the function of AURKA.

Overexpression of AURKA induces tumorigenesis, metastasis, and chemoresistance, which correlate with its pro-survival function in cancer cells. Thus, AURKA is thought to be an oncoprotein and a promising molecular target for cancer therapy. AURKA inhibitors, VX-680 (24) or MLN8054 (25), have shown anti-tumor activity against various aspects of tumor progression. Loss of SMAD4 is a genetically late event that occurs at the transition to malignancy, concurrent with the onset of invasive growth. Despite extensive knowledge regarding the biochemical properties of SMAD4, little is known about how the loss of SMAD4 function contributes to the tumorigenic process. Inactivation of SMAD4 has been correlated with increased invasiveness or the metastatic ability of human cancer cells, which is reminiscent of the phenotypes induced by overexpression of AURKA. Because our initial data from

different cancer cell lines indicated a reciprocal relationship between the expression of SMAD4 and AURKA and showed higher β-catenin expression in cells with AURKA to SMAD4 ratio greater than 1, the goal of this study is to explore the functional relationship among SMAD4, AURKA, and β-catenin signaling, and to understand their effect on tumor progression. Using mouse embryonic fibroblast cells and human cancer cell lines, we confirmed that SMAD4 has a potential suppressive function against AURKA-induced anchorage-independent growth, migration, and invasion of AGS, SW480, and HeLa cells. We selected these cell lines for 3 different reasons. First, in AGS cells, the expression ratio of AURKA to SMAD4 is greater than 1, and AURKA has been shown to activate the WNT/β-catenin pathway through GSK-3β phosphorylation (26). Second, in SW480 cells, SMAD4 protein expression is deficient and the restoration of SMAD4 suppressed WNT/β-catenin signal activity (11, 45). Third, although the expression ratio of AURKA to SMAD4 is less than 1, the oncogenic activity of AURKA in HeLa cells has been reported (46). Western blot analysis, qRT-PCR, and a luciferase activity assay using the 3 different cell lines clearly showed that SMAD4 transfection decreased both exogenous and endogenous AURKA expression in these cells, suggesting an inverse relationship between SMAD4 and AURKA. Consistent with our results shown in **Figure 7A**, three previous research papers (32, 47, 48), one of which had been reported by our research group, had shown that in contrast to remarkable increase in AURKA protein expression, SMAD4 protein expression decreased dramatically in advanced carcinoma stage of human gastric cancer. Although mRNA expression of *AURKA* existed in dysplasia stage samples (data not shown), AURKA protein levels were suppressed by SMAD4. Also, we validated that highly frequent oncogenic β-catenin mutations took place, allowing for aberrant oncogenic

activation of the β-catenin signaling pathway in TCGA tumor samples of diverse human cancer types, including gastric cancer (**Fig. 7D**). These data corroborate the findings in this study. These results also suggest that the β-catenin signaling is involved in carcinogenesis by virtue of its activation due to oncogenic mutations or AURKA activation.

AURKA is a well characterized oncoprotein that is overexpressed in a wide range of human cancers (30). Overexpression of active AURKA results in abnormal centrosome amplification (49) , which is reminiscent of a phenotype induced by deletion of the tumor suppressor TP53 (50). TP53 has been reported to directly interact with the N-terminal Aurora box of AURKA, thereby suppressing AURKA-mediated centrosome amplification and cellular transformation (51). Tumor progression occurs through the loss of function of diverse classes of tumor suppressor genes, thereby allowing amplification of oncogenic signals. Activation or restoration of one or more tumor suppressor proteins may counterbalance the overactivation of AURKA and inhibit the neoplastic transformation of cells. While activation of TP53 tumor suppressor protein is known to decrease AURKA-mediated cellular transformation, the role of the SMAD4 tumor suppressor protein in regulating AURKA has not been investigated. In our study, we found that the SMAD4 linker domain interacted with the AURKA C-terminal domain and reduced the expression of AURKA via Ub-dependent proteasomal degradation**.** While it has been reported that AURKA turnover is mediated through the APC-Ub-proteasome pathway (52), the mechanisms underlying proteasomal degradation of AURKA upon overexpression of SMAD4 require further investigation. While TP53 regulates AURKA by binding to the N-terminal domain of AURKA (51), we found that SMAD4 regulates AURKA function by binding to its C-terminal domain.

The C-terminus of AURKA harbors a kinase domain that is required for abnormal cellular transformation induced by AURKA (18). Thus, the involvement of this kinase domain in the binding of AURKA to SMAD4 may lead to functional inactivation of AURKA (**Fig. 7E**).

It has been reported that constitutive activation of AURKA as a result of activation of oncogenic RAS (13) and subsequent activation of the MAPK pathway (14) rather than cell cycle phase-specific expression occurred commonly in cancer cells. Although a detailed mechanism remains unclear, our data suggested that overexpression of SMAD4 did not affect expression of the AURKA mRNA transcript but reduced AURKA protein expression, independently with cell cycle. In normal tissues, AURKA was mainly localized to centrosome, but in malignant tissues, AURKA showed additional staining in cytoplasm. Immunohistochemical analysis revealed that AURKA overexpression was frequently found in the cytoplasmic region in cancer cell (40, 53). Moreover, some reports suggested that AURKA overexpression is likely to target cytoplasmic substrates related to oncogenic transformation, such as h-CPEB (54) and GSK-3β (26). These reports demonstrated that constitutive phosphorylation of AURKA maybe the reason of inducing its stabilization and consequent activation in cytoplasm (12). Our data demonstrated that SMAD4 bound to AURKA in cytoplasm, thereby inducing proteasomal degradation of AURKA.

An upstream kinase involved in regulating β-catenin signaling is GSK-3β, which promotes phosphorylation-dependent degradation of β-catenin and the linkage of the canonical WNT/β-catenin pathway and the PI3K/AKT signaling pathway (28). In addition, AURKA directly phosphorylates GSK-3β, thereby inactivating GSK-3β and enhancing nuclear accumulation of β-catenin and the activation of β-catenin/TCF

downstream target genes, such as *MYC*, *CCND1*, and *PLAUR* (26). In agreement with previous studies, our results showed that AURKA transfection increased AKT and GSK-3β phosphorylation, thereby inducing β-catenin/TCF transcriptional activity and increasing the expression of β-catenin target genes involved in tumor progression. Here, our results support the hypothesis that this oncogenic effect of AURKA was abrogated in part by transfecting cells with SMAD4. These data suggest that SMAD4-mediated downregulation of AURKA leads to suppression of WNT/β-catenin signaling and inhibition of the proliferation, migration, and invasion of cancer cells.

We examined whether the presence of AURKA influenced the tumor-suppressive function of SMAD4. Overexpression of SMAD4 in AGS and SW480 cells showed that SMAD4 suppressed the migration and invasion of these cancer cells. Interestingly, AURKA co-transfection with SMAD4 in these cells resulted in sufficient abrogation of the suppressive effect of SMAD4 on tumorigenicity and the WNT/β-catenin pathway. In contrast, *AURKA* siRNA co-transfection with *SMAD4* showed repression of the β-catenin pathway and tumor progression, similar to that caused by *SMAD4* transfection. These results suggested a predominant role for AURKA in SMAD4-mediated suppression of the WNT/β-catenin pathway and tumorigenicity. Overall, our study showed that the tumor-suppressive function of SMAD4 is mediated in part by AURKA. Understanding the molecular mechanisms underlying SMAD4-mediated inactivation of AURKA warrants further investigation.

Since SMAD4 is a common mediator of TGF-β-induced signals, an intriguing question is whether the inactivation of AURKA and the resultant downregulation of β-catenin signaling in AGS and SW480 cells upon overexpression of SMAD4 are dependent on TGF-β stimulation. It has been reported that SMAD4 being a signal

mediator of TGF-β can elicit cellular functions independent of TGF-β stimulation (3, 4, 44, 45). For instance, the restoration of SMAD4, independent of TGF-β induction, in Hs766T (4) or SW480 cells (44) has been reported to block their ability to grow progressively as tumors *in vivo*. In addition, the expression of claudin-1, a β-catenin target gene, was decreased in SMAD4 overexpressed SW480 colon cancer cells (45), independently of TGF-β stimulation. Consistent with previous studies, we identified a novel TGF-β-independent role of SMAD4 in the regulation of AURKA stability and β-catenin signaling in cancer cells. Moreover, SMAD4 has been reported to inhibit RAS-dependent ERK activity in RAS-transformed keratinocytes (29). Since AURKA is a substrate of ERK (14), the possibility that SMAD4 can inhibit AURKA through inactivation of upstream RAS-ERK signaling cannot be ruled out.

Taken together, our findings that SMAD4 interacts with AURKA and downregulates AURKA function, resulting in reduction of β-catenin signaling and tumor progression, provide a novel mechanism for tumor-suppressive function of SMAD4.

Disclosure of Potential Conflicts of Interest

No potential conflicts of interest were disclosed.

Acknowledgments

We would like to thank Da-Hye Ko, Hyung Suk Kim, and Ga Ryeong Kim for their technical assistance.

Authors' Contributions

Conception and design: Lina Jia, Hun Seok Lee, Young Kee Shin

Development of methodology: Lina Jia, Hun Seok Lee, Chun Fu Wu, Juthika Kundu, Sang Gyu Park, Young Kee Shin

Acquisition of data: Lina Jia, Hun Seok Lee, Young Kee Shin

Analysis and interpretation of data: Lina Jia, Hun Seok Lee, Sang Gyu Park, Ryong Nam Kim, Li-Hui Wang, Özgür Cem Erkin, Jong-Sun Choi, Young Kee Shin

Writing, review, and/or revision of the manuscript: Lina Jia, Hun Seok Lee, Juthika Kundu, Sang Gyu Park, Ryong Nam Kim, Young Kee Shin

Administrative, technical, or material support: Lina Jia, Hun Seok Lee, Sang Gyu Park, Seoung Wan Chae, Ho Bin Yang, Yoon-La Choi, Young Kee Shin

Study supervision: Young Kee Shin

Grant Support

This research was supported by the R&D Program for Society of the National Research Foundation (NRF) funded by the Ministry of Science, ICT & Future Planning (Grant number: NRF-2013M3C8A1078433) and by the Global Core Research Center (GCRC) grant (Grant number: 2012-0001194) from the National Research Foundation (NRF), Ministry of Education, Science and Technology (MEST), Republic of Korea.

Reference

1. Hahn SA, Schutte M, Hoque AT, Moskaluk CA, da Costa LT, Rozenblum E, et al. DPC4, a candidate tumor suppressor gene at human chromosome 18q21.1. Science. 1996;271:350-3.
2. Candia AF, Watabe T, Hawley SH, Onichtchouk D, Zhang Y, Derynck R, et al. Cellular interpretation of multiple TGF-beta signals: intracellular antagonism between activin/BVg1 and BMP-2/4 signaling mediated by Smads. Development. 1997;124:4467-80.
3. Schwarte-Waldhoff I, Klein S, Blass-Kampmann S, Hintelmann A, Eilert C, Dreschers S, et al. DPC4/SMAD4 mediated tumor suppression of colon carcinoma cells is associated with reduced urokinase expression. Oncogene. 1999;18:3152-8.
4. Schwarte-Waldhoff I, Volpert OV, Bouck NP, Sipos B, Hahn SA, Klein-Scory S, et al. Smad4/DPC4-mediated tumor suppression through suppression of angiogenesis. Proceedings of the National Academy of Sciences of the United States of America. 2000;97:9624-9.
5. Reinacher-Schick A, Baldus SE, Romdhana B, Landsberg S, Zapatka M, Monig SP, et al. Loss of Smad4 correlates with loss of the invasion suppressor E-cadherin in advanced colorectal carcinomas. The Journal of pathology. 2004;202:412-20.
6. Freeman TJ, Smith JJ, Chen X, Washington MK, Roland JT, Means AL, et al. Smad4-mediated signaling inhibits intestinal neoplasia by inhibiting expression of beta-catenin. Gastroenterology. 2012;142:562-71 e2.
7. He TC, Sparks AB, Rago C, Hermeking H, Zawel L, da Costa LT, et al. Identification of c-MYC as a target of the APC pathway. Science. 1998;281:1509-12.
8. Shtutman M, Zhurinsky J, Simcha I, Albanese C, D'Amico M, Pestell R, et al. The cyclin D1 gene is a target of the beta-catenin/LEF-1 pathway. Proceedings of the National Academy of Sciences of the United States of America. 1999;96:5522-7.
9. Tetsu O, McCormick F. Beta-catenin regulates expression of cyclin D1 in colon carcinoma cells. Nature. 1999;398:422-6.
10. Kundu JK, Choi KY, Surh YJ. beta-Catenin-mediated signaling: a novel molecular target for chemoprevention with anti-inflammatory substances. Biochimica et biophysica acta. 2006;1765:14-24.
11. Tian X, Du H, Fu X, Li K, Li A, Zhang Y. Smad4 restoration leads to a suppression of Wnt/beta-catenin signaling activity and migration capacity in human colon carcinoma cells. Biochemical and biophysical research communications. 2009;380:478-83.
12. Kitajima S, Kudo Y, Ogawa I, Tatsuka M, Kawai H, Pagano M, et al. Constitutive phosphorylation of aurora-a on ser51 induces its stabilization and consequent overexpression in cancer. PLoS One. 2007;2:e944.
13. Tatsuka M, Sato S, Kitajima S, Suto S, Kawai H, Miyauchi M, et al. Overexpression of Aurora-A potentiates HRAS-mediated oncogenic transformation and is implicated in oral carcinogenesis. Oncogene. 2005;24:1122-7.

14. Furukawa T, Kanai N, Shiwaku HO, Soga N, Uehara A, Horii A. AURKA is one of the downstream targets of MAPK1/ERK2 in pancreatic cancer. Oncogene. 2006;25:4831-9.
15. Miyoshi Y, Iwao K, Egawa C, Noguchi S. Association of centrosomal kinase STK15/BTAK mRNA expression with chromosomal instability in human breast cancers. International journal of cancer Journal international du cancer. 2001;92:370-3.
16. Gritsko TM, Coppola D, Paciga JE, Yang L, Sun M, Shelley SA, et al. Activation and overexpression of centrosome kinase BTAK/Aurora-A in human ovarian cancer. Clinical cancer research : an official journal of the American Association for Cancer Research. 2003;9:1420-6.
17. Li D, Zhu J, Firozi PF, Abbruzzese JL, Evans DB, Cleary K, et al. Overexpression of oncogenic STK15/BTAK/Aurora A kinase in human pancreatic cancer. Clinical cancer research : an official journal of the American Association for Cancer Research. 2003;9:991-7.
18. Bischoff JR, Anderson L, Zhu Y, Mossie K, Ng L, Souza B, et al. A homologue of Drosophila aurora kinase is oncogenic and amplified in human colorectal cancers. The EMBO journal. 1998;17:3052-65.
19. Sen S, Zhou H, Zhang RD, Yoon DS, Vakar-Lopez F, Ito S, et al. Amplification/overexpression of a mitotic kinase gene in human bladder cancer. Journal of the National Cancer Institute. 2002;94:1320-9.
20. Tong T, Zhong Y, Kong J, Dong L, Song Y, Fu M, et al. Overexpression of Aurora-A contributes to malignant development of human esophageal squamous cell carcinoma. Clinical cancer research : an official journal of the American Association for Cancer Research. 2004;10:7304-10.
21. Yao JE, Yan M, Guan Z, Pan CB, Xia LP, Li CX, et al. Aurora-A down-regulates IkappaBalpha via Akt activation and interacts with insulin-like growth factor-1 induced phosphatidylinositol 3-kinase pathway for cancer cell survival. Molecular cancer. 2009;8:95.
22. Dar AA, Belkhiri A, Ecsedy J, Zaika A, El-Rifai W. Aurora kinase A inhibition leads to p73-dependent apoptosis in p53-deficient cancer cells. Cancer research. 2008;68:8998-9004.
23. Ulisse S, Arlot-Bonnemains Y, Baldini E, Morrone S, Carocci S, Di Luigi L, et al. Inhibition of the aurora kinases suppresses in vitro NT2-D1 cell growth and tumorigenicity. The Journal of endocrinology. 2010;204:135-42.
24. Harrington EA, Bebbington D, Moore J, Rasmussen RK, Ajose-Adeogun AO, Nakayama T, et al. VX-680, a potent and selective small-molecule inhibitor of the Aurora kinases, suppresses tumor growth in vivo. Nature medicine. 2004;10:262-7.
25. Huck JJ, Zhang M, McDonald A, Bowman D, Hoar KM, Stringer B, et al. MLN8054, an inhibitor of Aurora A kinase, induces senescence in human tumor cells both in vitro and in vivo. Molecular cancer research : MCR. 2010;8:373-84.
26. Dar AA, Belkhiri A, El-Rifai W. The aurora kinase A regulates GSK-3beta in gastric cancer cells. Oncogene. 2009;28:866-75.
27. Yang H, He L, Kruk P, Nicosia SV, Cheng JQ. Aurora-A induces cell survival and

chemoresistance by activation of Akt through a p53-dependent manner in ovarian cancer cells. International journal of cancer Journal international du cancer. 2006;119:2304-12.

28. Fukumoto S, Hsieh CM, Maemura K, Layne MD, Yet SF, Lee KH, et al. Akt participation in the Wnt signaling pathway through Dishevelled. The Journal of biological chemistry. 2001;276:17479-83.

29. Iglesias M, Frontelo P, Gamallo C, Quintanilla M. Blockade of Smad4 in transformed keratinocytes containing a Ras oncogene leads to hyperactivation of the Ras-dependent Erk signalling pathway associated with progression to undifferentiated carcinomas. Oncogene. 2000;19:4134-45.

30. Marumoto T, Zhang D, Saya H. Aurora-A - a guardian of poles. Nature reviews Cancer. 2005;5:42-50.

31. Wang LH, Kim SH, Lee JH, Choi YL, Kim YC, Park TS, et al. Inactivation of SMAD4 tumor suppressor gene during gastric carcinoma progression. Clinical cancer research : an official journal of the American Association for Cancer Research. 2007;13:102-10.

32. Kim SH, Lee SH, Choi YL, Wang LH, Park CK, Shin YK. Extensive alteration in the expression profiles of TGFB pathway signaling components and TP53 is observed along the gastric dysplasia-carcinoma sequence. Histology and histopathology. 2008;23:1439-52.

33. Dai JL, Bansal RK, Kern SE. G1 cell cycle arrest and apoptosis induction by nuclear Smad4/Dpc4: phenotypes reversed by a tumorigenic mutation. Proceedings of the National Academy of Sciences of the United States of America. 1999;96:1427-32.

34. He L, Yang H, Ma Y, Pledger WJ, Cress WD, Cheng JQ. Identification of Aurora-A as a direct target of E2F3 during G2/M cell cycle progression. The Journal of biological chemistry. 2008;283:31012-20.

35. Gorgun G, Calabrese E, Hideshima T, Ecsedy J, Perrone G, Mani M, et al. A novel Aurora-A kinase inhibitor MLN8237 induces cytotoxicity and cell-cycle arrest in multiple myeloma. Blood. 2010;115:5202-13.

36. Hu CD, Chinenov Y, Kerppola TK. Visualization of interactions among bZIP and Rel family proteins in living cells using bimolecular fluorescence complementation. Mol Cell. 2002;9:789-98.

37. Kerppola TK. Design and implementation of bimolecular fluorescence complementation (BiFC) assays for the visualization of protein interactions in living cells. Nature protocols. 2006;1:1278-86.

38. Saka Y, Hagemann AI, Piepenburg O, Smith JC. Nuclear accumulation of Smad complexes occurs only after the midblastula transition in Xenopus. Development. 2007;134:4209-18.

39. Inman GJ, Nicolas FJ, Hill CS. Nucleocytoplasmic shuttling of Smads 2, 3, and 4 permits sensing of TGF-beta receptor activity. Mol Cell. 2002;10:283-94.

40. Burum-Auensen E, De Angelis PM, Schjolberg AR, Kravik KL, Aure M, Clausen OP.

Subcellular localization of the spindle proteins Aurora A, Mad2, and BUBR1 assessed by immunohistochemistry. J Histochem Cytochem. 2007;55:477-86.

41. Behrens J, von Kries JP, Kuhl M, Bruhn L, Wedlich D, Grosschedl R, et al. Functional interaction of beta-catenin with the transcription factor LEF-1. Nature. 1996;382:638-42.

42. Katuri V, Tang Y, Marshall B, Rashid A, Jogunoori W, Volpe EA, et al. Inactivation of ELF/TGF-beta signaling in human gastrointestinal cancer. Oncogene. 2005;24:8012-24.

43. Tojo M, Hamashima Y, Hanyu A, Kajimoto T, Saitoh M, Miyazono K, et al. The ALK-5 inhibitor A-83-01 inhibits Smad signaling and epithelial-to-mesenchymal transition by transforming growth factor-beta. Cancer science. 2005;96:791-800.

44. Muller N, Reinacher-Schick A, Baldus S, van Hengel J, Berx G, Baar A, et al. Smad4 induces the tumor suppressor E-cadherin and P-cadherin in colon carcinoma cells. Oncogene. 2002;21:6049-58.

45. Shiou SR, Singh AB, Moorthy K, Datta PK, Washington MK, Beauchamp RD, et al. Smad4 regulates claudin-1 expression in a transforming growth factor-beta-independent manner in colon cancer cells. Cancer research. 2007;67:1571-9.

46. Meraldi P, Honda R, Nigg EA. Aurora-A overexpression reveals tetraploidization as a major route to centrosome amplification in p53-/- cells. The EMBO journal. 2002;21:483-92.

47. Xu X, Xiao J, Wei S, Xie X, Huang Y, Tian X, et al. Relationship between expression of Aurka and clinicopathological characteristics in gastric cancer patients. Health. 2014;6:243-9.

48. Scarpini S, Roupret M, Renard-Penna R, Camparo P, Cussenot O, Comperat E. Impact of the expression of Aurora-A, p53, and MIB-1 on the prognosis of urothelial carcinomas of the upper urinary tract. Urologic oncology. 2012;30:182-7.

49. Zhou H, Kuang J, Zhong L, Kuo WL, Gray JW, Sahin A, et al. Tumour amplified kinase STK15/BTAK induces centrosome amplification, aneuploidy and transformation. Nature genetics. 1998;20:189-93.

50. Fukasawa K, Choi T, Kuriyama R, Rulong S, Vande Woude GF. Abnormal centrosome amplification in the absence of p53. Science. 1996;271:1744-7.

51. Chen SS, Chang PC, Cheng YW, Tang FM, Lin YS. Suppression of the STK15 oncogenic activity requires a transactivation-independent p53 function. The EMBO journal. 2002;21:4491-9.

52. Taguchi S, Honda K, Sugiura K, Yamaguchi A, Furukawa K, Urano T. Degradation of human Aurora-A protein kinase is mediated by hCdh1. FEBS letters. 2002;519:59-65.

53. Ogawa E, Takenaka K, Katakura H, Adachi M, Otake Y, Toda Y, et al. Perimembrane Aurora-A expression is a significant prognostic factor in correlation with proliferative activity in non-small-cell lung cancer (NSCLC). Ann Surg Oncol. 2008;15:547-54.

54. Sasayama T, Marumoto T, Kunitoku N, Zhang D, Tamaki N, Kohmura E, et al. Over-expression of Aurora-A targets cytoplasmic polyadenylation element binding protein and promotes mRNA polyadenylation of Cdk1 and cyclin B1. Genes Cells. 2005;10:627-38.

1

Figure legends

Fig. 1. SMAD4 inversely regulates AURKA function in carcinogenesis.

(A) Western blotting analysis of AURKA, SMAD4, and β-catenin in a variety of cells. The names of cell lines from which the protein was extracted are indicated.

(B) The representative micrographs of the cell colonies, formed in soft agar by TPA-stimulated AURKA-NIH3T3 cells transfected with or without 6*Myc*-*SMAD4*. Scale bar, 100 μm. After 4 weeks, the colonies were counted. The graphs show the colony formation efficiencies expressed as colony numbers/field. Data were presented as means ±SD obtained from 5 random areas from three independent experiments (*, vs. vector control; †, AURKA-NIH3T3+SMAD4 vs. AURKA-NIH3T3). *P<0.001 and †P<0.001.

(C and D) AGS, SW480, and HeLa cells were transfected with indicated combinations of plasmids encoding 6*Myc*-SMAD4 or *FLAG*-AURKA for 24 h and subjected to cell migration and invasion assay (n=3). Data were presented as means ±SD obtained from three independent experiments (*, vs. vector control; †, vs. AURKA; ‡, vs. AURKA+SMAD4). *P<0.05, †P<0.05, and ‡P<0.05.

(E and F) HeLa cells transfected with empty vector, SMAD4, AURKA, or a combination for 36 h and treated with MLN8237 (100 nM) or DMSO were synchronized with DTB. The cell distribution at 8 h of release from DTB were subjected to flow cytometry (*, vs. vector control; †, vs. AURKA; ‡, vs. AURKA+SMAD4). *P<0.001, †P<0.001, and ‡P<0.001.

Fig. 2. SMAD4 inhibits the expression of AURKA via proteasomal degradation.

(A) AGS, SW480, HeLa, and HaCaT cells were transfected with either increasing

amounts of 6*Myc*-*SMAD4* (3 or 5 μg) or empty vector. SMAD4 and AURKA were blotted with specific antibodies. ACTB was used as the loading control.

(B) AGS and HeLa cells were transfected with either control siRNA or *SMAD4* siRNA (5 or 10 nM) for 24 h. Total cells lysate was harvested and the levels of endogenous SMAD4 and AURKA were blotted with specific antibodies. ACTB was used as the loading control.

(C) HeLa cells were transfected with either increasing amounts of 6*Myc*-*SMAD4* (3 or 5 μg) or empty vector for 36 h, and treated with MG132 (10 μM) or DMSO for 12 h before harvesting. Cells lysate was analyzed with anti-SMAD4, anti-AURKA, anti-β-catenin, and anti-ACTB antibodies.

(D) HeLa cells were co-transfected with the indicated combinations of plasmids encoding 6*Myc*-SMAD4, *HA*-Ub or *FLAG*-AURKA for 36 h, and treated with MG132 (10 μM) or DMSO for 4 h before harvesting. Ubiquitination assay was performed as described in the Materials and Methods section, and then analyzed using anti-*HA*-HRP, anti-*Myc* and anti-*FLAG*-HRP antibodies.

Fig. 3. SMAD4 interacts with AURKA.

(A) Physical interaction between endogenous SMAD4 and AURKA. Cells lysate (Lysate) was obtained from HeLa cells and immunoprecipitated with either anti-AURKA antibody and normal goat IgG (left) or anti-SMAD4 antibody and normal mouse IgG (right). The immunoprecipitates were blotted with anti-SMAD4 antibody, anti-SMAD2 antibody, or anti-AURKA antibody.

(B) Visualization of SMAD4 and AURKA interactions in HeLa cells using BiFC analysis. Top panel: HeLa cells were co-transfected with the plasmid encoding *FLAG*-

AURKA-VN173 (AURKA) and either the plasmid encoding full form *HA*-SMAD4-VC155 (Full) or *HA*-SMAD4-VC155 truncated mutants (MH1, Linker, and MH2). Middle panel: HeLa cells were co-transfected with the plasmid encoding *HA*-SMAD4-VC155 (SMAD4) and either the plasmid encoding full form *FLAG*-AURKA-VN173 (Full) or *FLAG*-AURKA-VN173 truncated mutants (C-terminus and N-terminus). Bottom panel: HeLa cells that co-expressed *HA*-SMAD4-VC155 and *FLAG*-SMAD2 (MH2)-VN173 were used as positive control or *HA*-SMAD4-VC155 and *FLAG*-SMAD2 (MH1) were used as negative control. Fluorescence images indicated in each panel were captured under fluorescence microscopy (×40) at 18 h after transfection. Scale bar, 5 μm.

(C) For the competition assay, HeLa cells were co-transfected with plasmids encoding *FLAG*-AURKA-VN173 and *HA*-SMAD4-VC155 in the absence or presence of co-transfection with the 3×*FLAG-AURKA* plasmid (0.5 or 1 μg). The fluorescence signal was captured under fluorescence microscopy (×10) and counted in 5 random areas. GFP-positive cells were normalized with total cell counts and represented counts/100 cells. Scale bar, 100 μm. Values are the means ±SD. ‡P<0.001. Expression of fusion proteins was determined by Western blotting with anti-*HA*, anti-*FLAG*-M2 and anti-ACTB antibodies.

(D) HeLa cells cultured in four-well chamber slides were fixed and incubated with a 1:100 dilution of mouse anti-SMAD4 and rabbit anti-AURKA antibody, PLA probe, ligase solution, and polymerase solution in order. Fluorescence on the mounted slides was captured with a confocal microscope system. Scale bar, 5 μm.

(E) HeLa cells cultured in eight-well chamber slides were fixed and incubated with a 1:50 dilution of mouse anti-SMAD4 and rabbit anti-AURKA antibody and then with the

appropriate secondary antibodies against mouse and rabbit IgG, conjugated with Alexa Fluor 488 and 546, respectively. Fluorescence on the mounted slides was captured with a confocal microscope system. Scale bar, 5 μm.

(F) HeLa cells were co-transfected with the plasmid encoding *FLAG*-AURKA-VN173 and either full form *HA*-SMAD4-VC155 or *HA*-SMAD4-VC155 truncated mutants. Cells lysate was immunoprecipitated with anti-*FLAG*-M2 antibody and blotted using the indicated antibodies.

(G) HeLa cells were co-transfected with the plasmid encoding *HA*-SMAD4-VC155 and either full form *FLAG*-AURKA-VN173 or *FLAG*-AURKA-VN173 truncated mutants. Cells lysate was immunoprecipitated with anti-*HA* antibody and blotted using the indicated antibodies.

(H) HeLa cells were co-transfected with the plasmid encoding *HA*-SMAD4-Linker-VC155 and *FLAG*-AURKA-C-teminal-VN173. Cells lysate was immunoprecipitated with anti-*FLAG*-M2 antibody and blotted using the indicated antibodies.

(I) HeLa cells were transfected with control vector or the plasmid encoding *HA*-SMAD4-VC155 or *HA*-SMAD4-Linker-VC155. Cells lysate blotted using the indicated antibodies

Fig. 4. SMAD4-mediated downregulation of AURKA leads to the inhibition of β-catenin signaling.

(A) AGS or SW480 cells were transfected with the indicated combinations of plasmids encoding 6*Myc*-SMAD4 or *FLAG*-AURKA. The downstream genes of AURKA and β-catenin were analyzed by Western blotting using special antibodies. ACTB was used as a control for protein loading.

(B) AGS or SW480 cells were co-transfected with a luciferase reporter gene driven by a pTOPFlash/pFOPFlash promoter and expression vectors for 3×*FLAG*-AURKA or 6*Myc*-SMAD4 as indicated. Luciferase reporter activity was measured and normalized to pRL-TK.

(C) qRT-PCR analysis of downstream genes of β-catenin in AGS or SW480 cells, including *PLAUR*, *CCND1*, and *MYC*. Total-RNA was isolated from AGS or SW480 cells transfected with the indicated combinations of plasmids encoding 6*Myc*-SMAD4 or *FLAG*-AURKA and amplified by RT-PCR with their specific primers. *HPRT* was used as a control. Data were presented as means ±SD obtained from three independent experiments (*, vs. vector control; †, vs. AURKA; ‡, vs. AURKA+SMAD4). *P<0.05, †P<0.05, and ‡P<0.05.

Fig. 5. AURKA is the direct target for SMAD4-induced suppression of the WNT/β-catenin pathway.

(A) AGS or SW480 cells were pretreated with control siRNA or *AURKA* siRNA (50 nM), and then transfected with the plasmid encoding 6*Myc*-SMAD4 or empty vector. The downstream genes of AURKA and β-catenin were analyzed by western blotting using specific antibodies. ACTB was used as a control for protein loading.

(B) AGS or SW480 cells were pretreated with control siRNA or *AURKA* siRNA (10 nM) for 48 h and co-transfected with a luciferase reporter gene driven by a pTOPFlash/pFOPFlash promoter and expression vectors for 6*Myc*-SMAD4 or empty vector as indicated. Luciferase reporter activity was measured and normalized to pRL-TK.

(C) The downstream genes of β-catenin were analyzed by qRT-PCR, including *PLAUR*,

CCND1, and *MYC*. Total RNA was isolated from AGS or SW480 cells that were transfected with control siRNA or *AURKA* siRNA (10 nM) for 48 h, and the plasmid encoding 6*Myc*-SMAD4 or empty vector was co-transfected for 24 h. *HPRT* was used as a control. Data were presented as means ±SD obtained from three independent experiments (**P*<0.05, †*P*<0.01, ‡*P*<0.001, compared to the control group).

Fig. 6. SMAD4-mediated repression of AURKA and β-catenin is independent of TGF-β signaling.

(A) AGS or SW480 cells were transfected with the plasmid encoding 6*Myc*-SMAD4 with empty vector or *FLAG*-TGF-βRII, 20 hours later, cells were treated, as indicated, with or without 45 nM A83-01 and 5 nM TGF-β1 and cultured for another 2 h before western blotting. Cells lysate was analyzed with anti-phospho-SMAD2/SMAD3, anti-SMAD2/SMAD3 and anti-ACTB antibodies.

(B) AGS or SW480 cells were transfected with the plasmid encoding 6*Myc*-SMAD4 with empty vector or *FLAG-TGF-βRII*, 20 hours later, cells were treated, as indicated, with or without 45 nM A83-01 and 5 nM TGF-β1 and cultured for another 2 h before Western blotting. The downstream genes of AURKA and β-catenin were analyzed by western blotting using specific antibodies. ACTB was used as a control for protein loading.

Fig. 7. TMA (tissue microarray) assay with immunohistochemistry of SMAD4 and AURKA protein expression and *AURKA* amplification, *SMAD4* deletion and β-catenin gene mutation across TCGA clinical tumor samples.

(A) SMAD4 and AURKA protein expressions were assayed in cytosols (top) and nuclei

(middle) of human stomach carcinoma, dysplasia and normal cells, and IHC images (bottom) are shown (magnification ×200).

(B) Left: *AURKA* amplification across diverse TCGA human cancer types. Right: *AURKA* amplification and its RNA expression in 219 TCGA stomach cancer samples.

(C) Left: *SMAD4* deletion across diverse TCGA human cancer types. Right: *SMAD4* deletion and its RNA expression in 219 TCGA stomach cancer samples.

(D) β-catenin gene mutation across diverse TCGA human cancer types.

(E) A schematic model showing the role of SMAD4 in the modulation of AURKA- and β-catenin-mediated signal transduction pathways and its impact on cancer cells survival. While upregulated SMAD4 expression blocks AURKA activation as defense mechanism against oncogenic addiction in dysplastic cell, AURKA activation with SMAD4 loss switches on β-catenin signaling in advanced cancer stage.

Fig. 1A

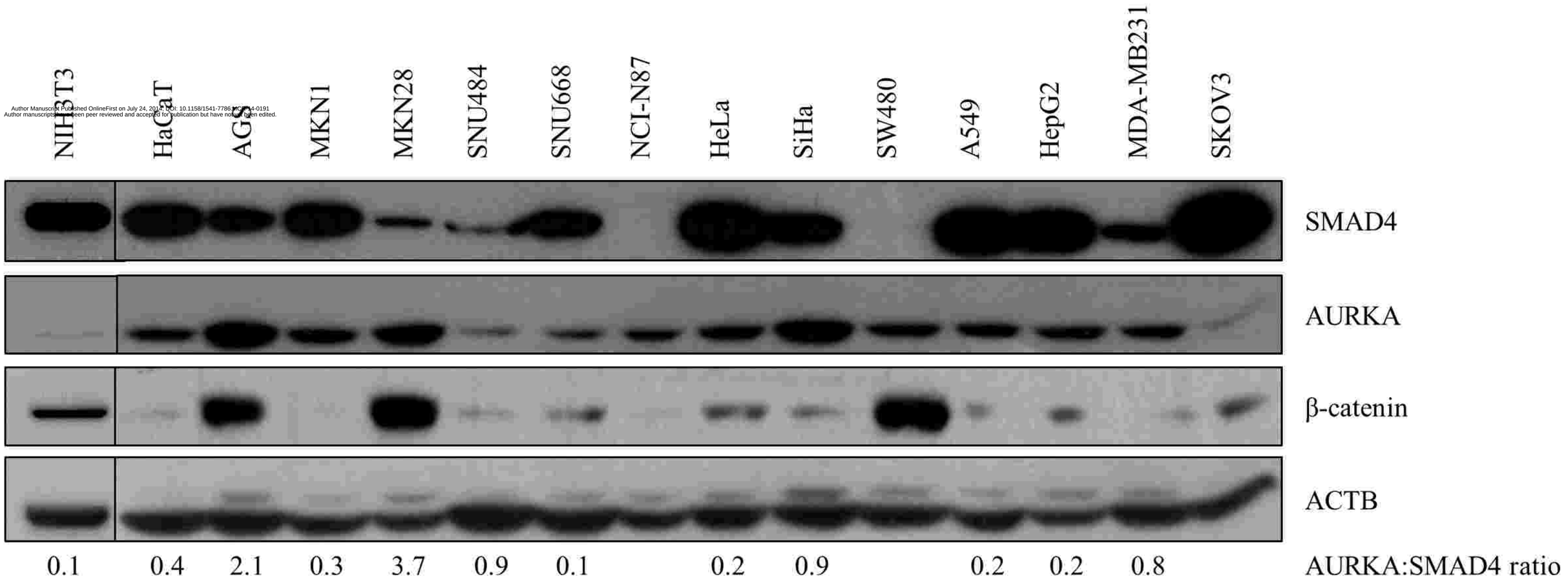

Fig. 1B

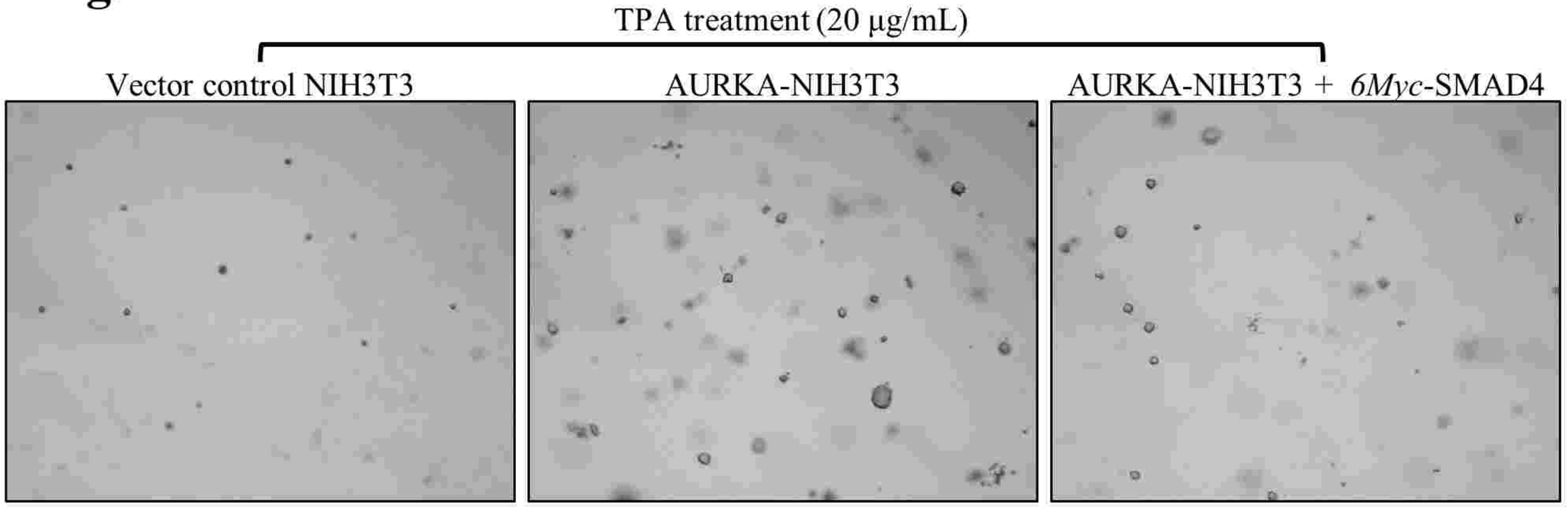

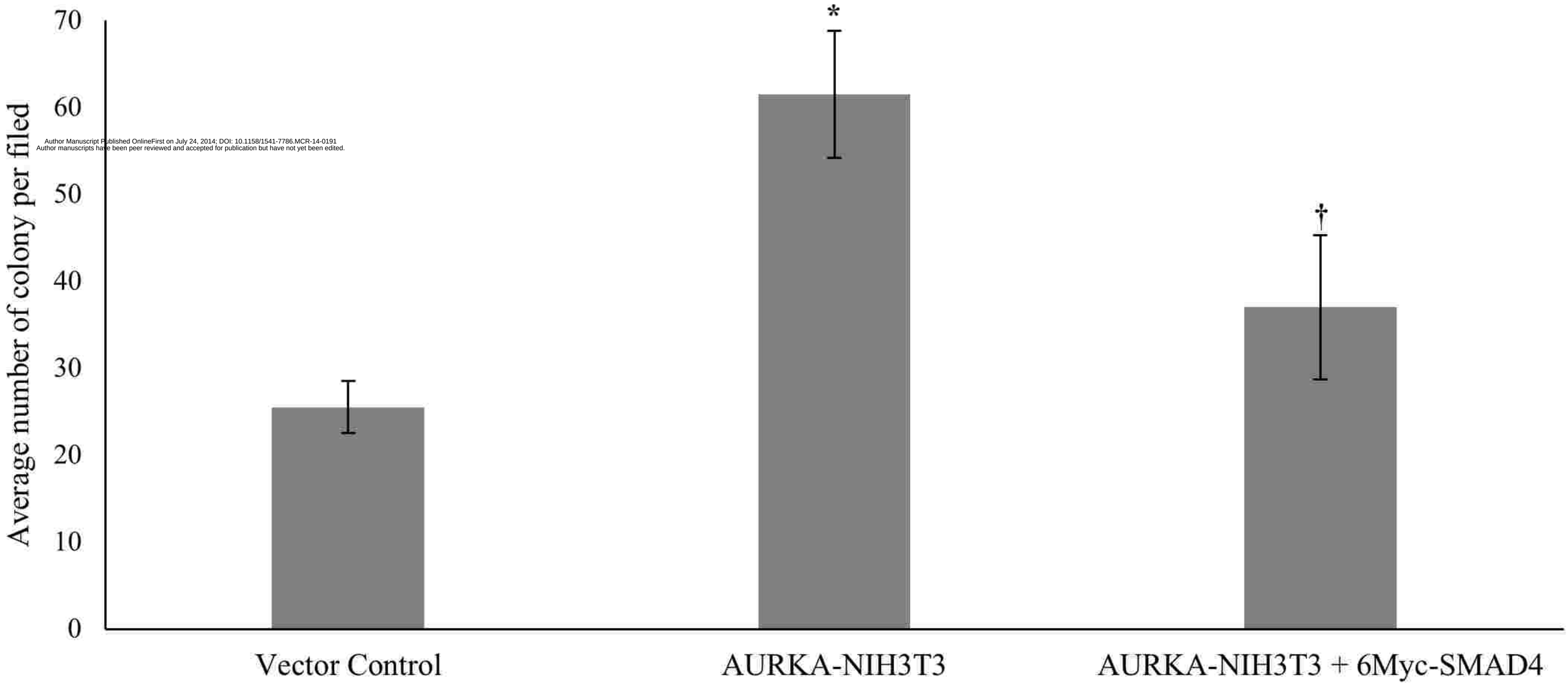

Author Manuscript Published OnlineFirst on July 24, 2014; DOI: 10.1158/1541-7786.MCR-14-0191
Author manuscripts have been peer reviewed and accepted for publication but have not yet been edited.

Fig. 1C

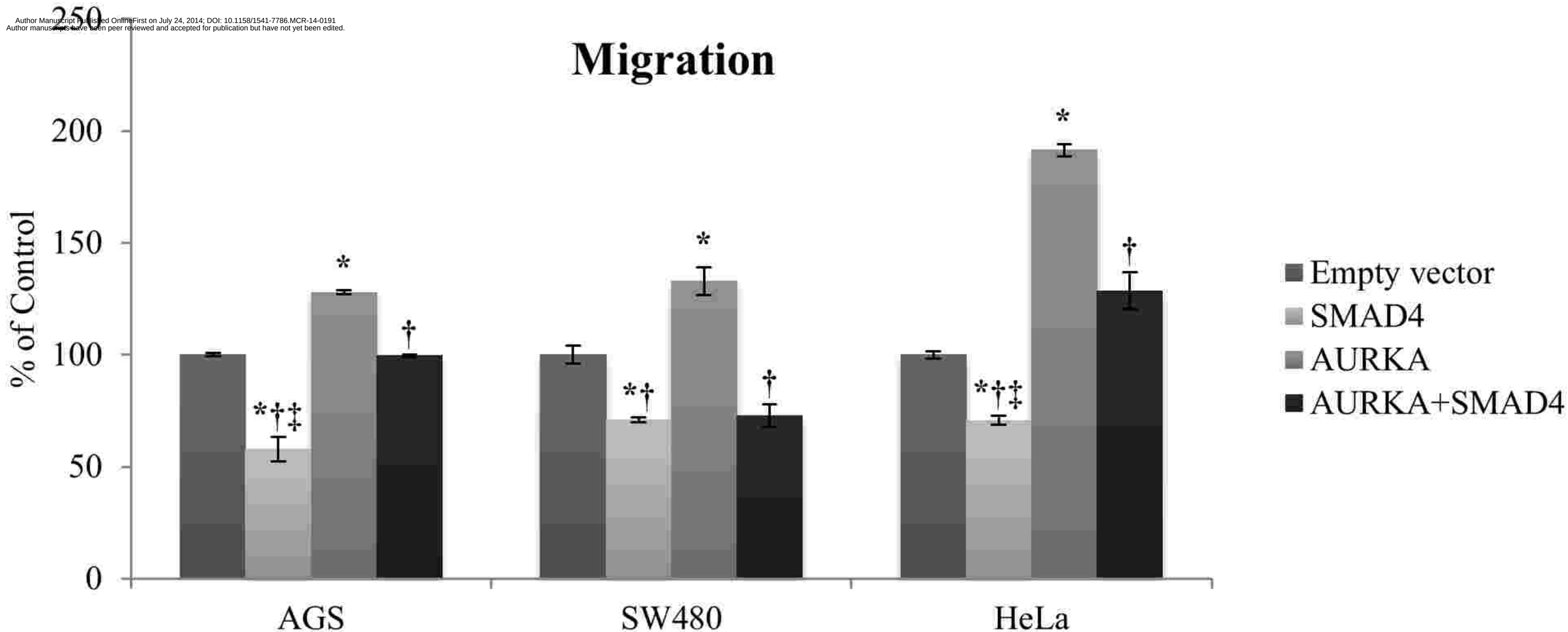

Fig. 1D

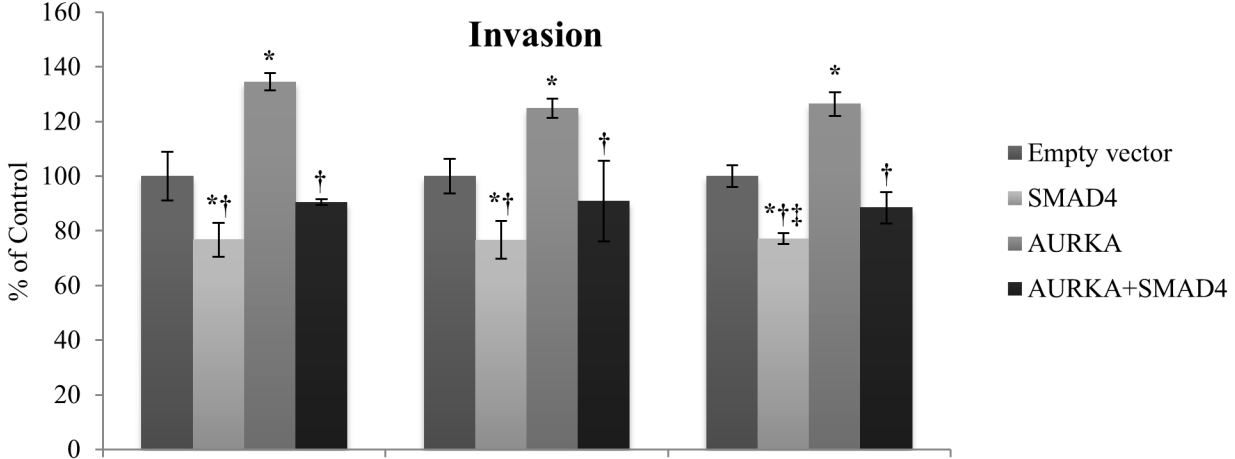

Fig. 1E

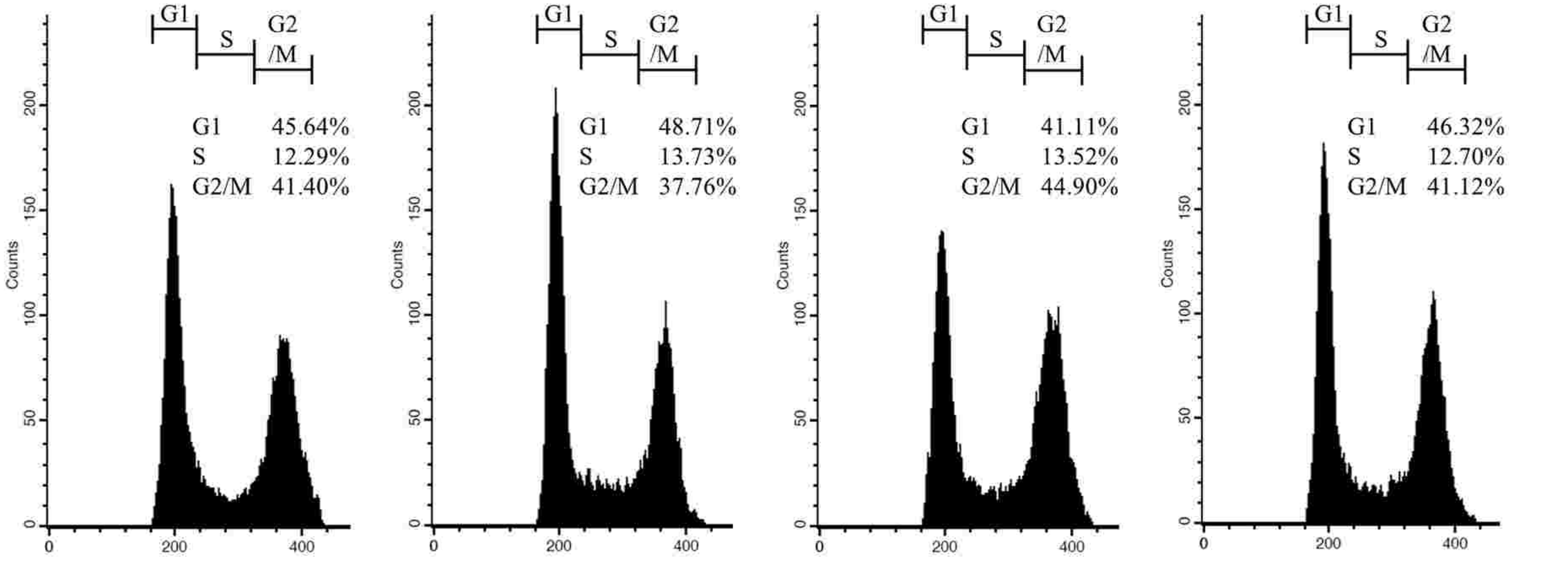

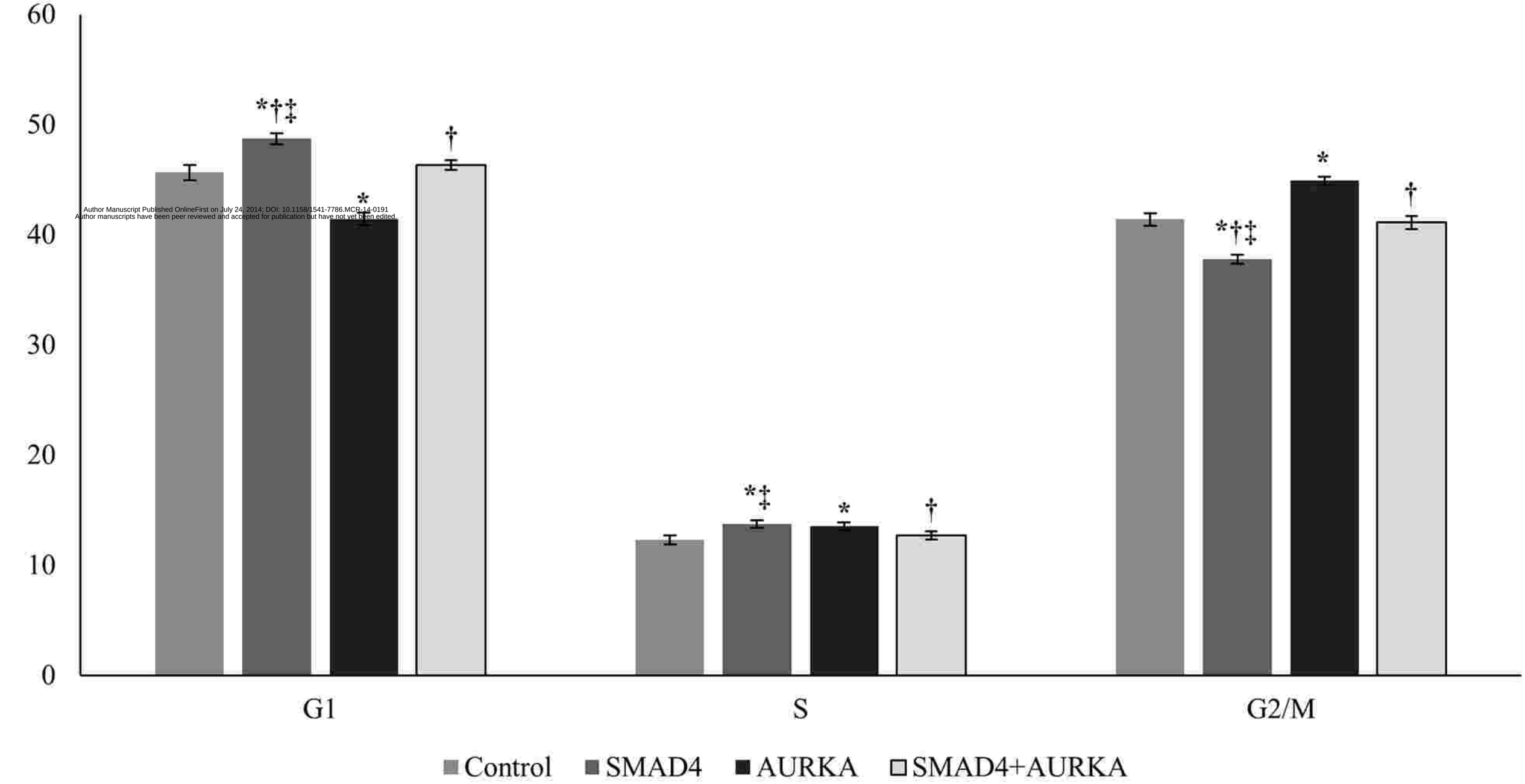

Author Manuscript Published OnlineFirst on July 24, 2014; DOI: 10.1158/1541-7786.MCR-14-0191
Author manuscripts have been peer reviewed and accepted for publication but have not yet been edited.

Fig. 1F

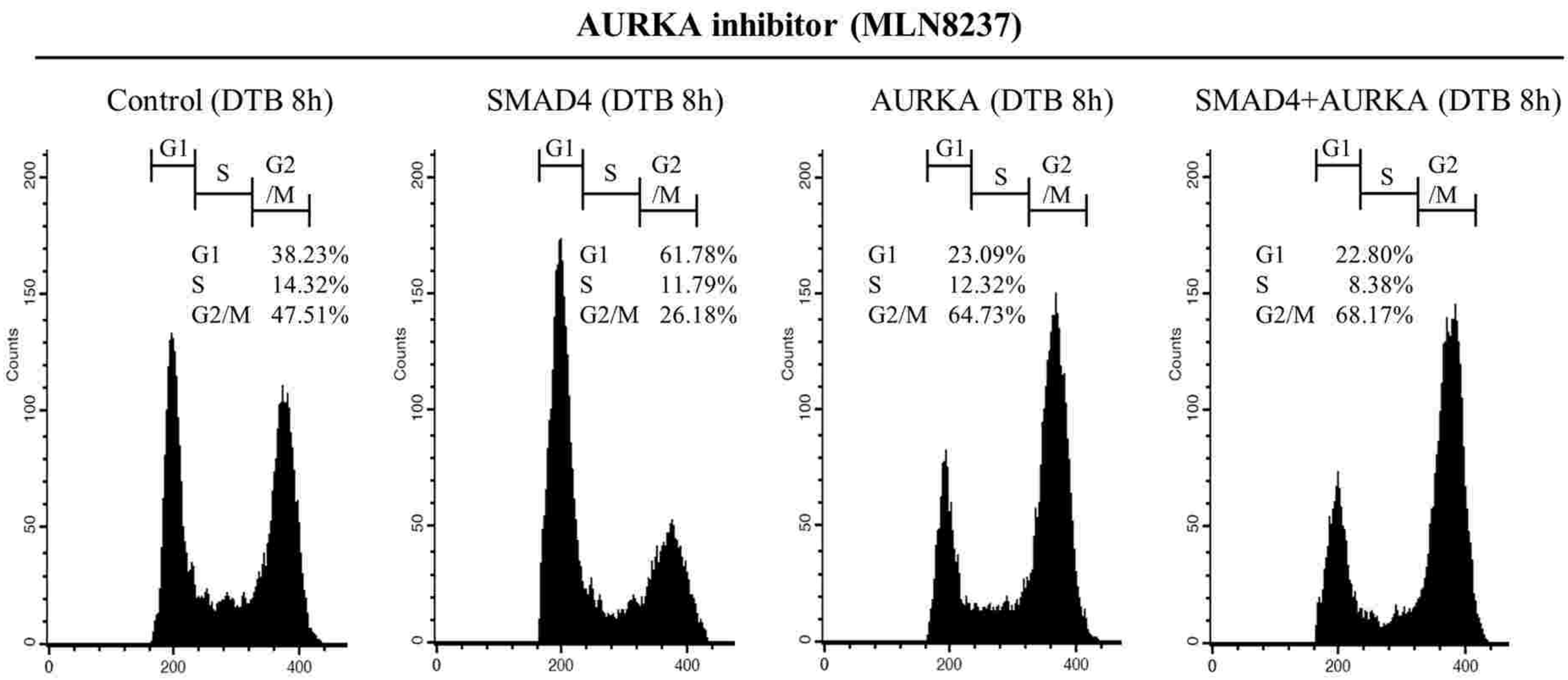

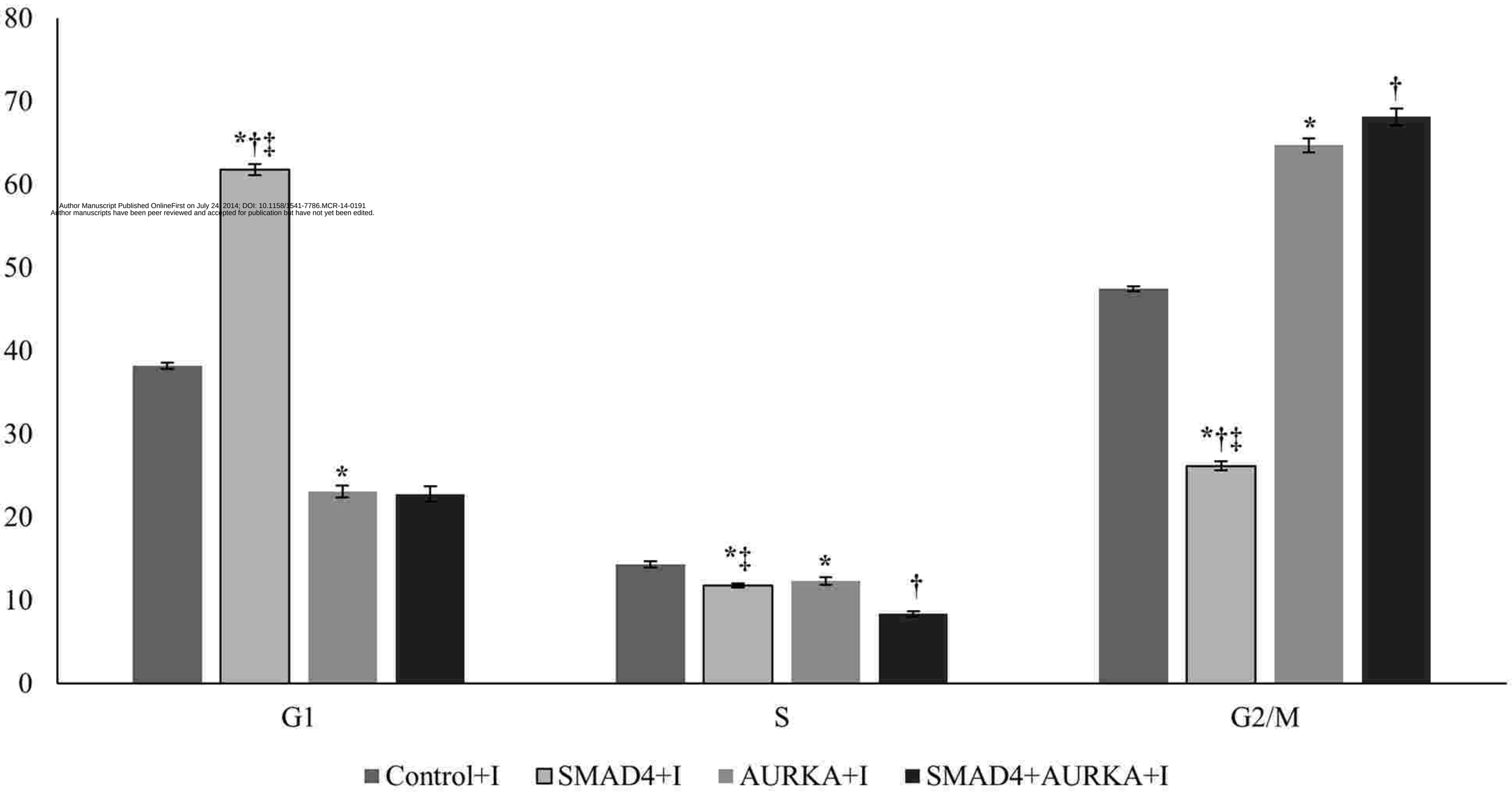

Fig. 2A

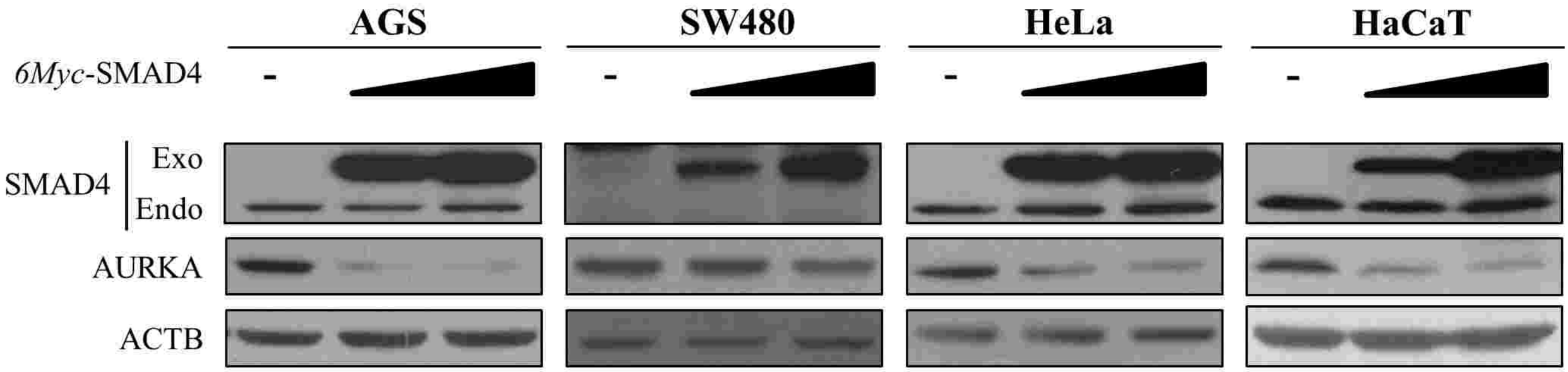

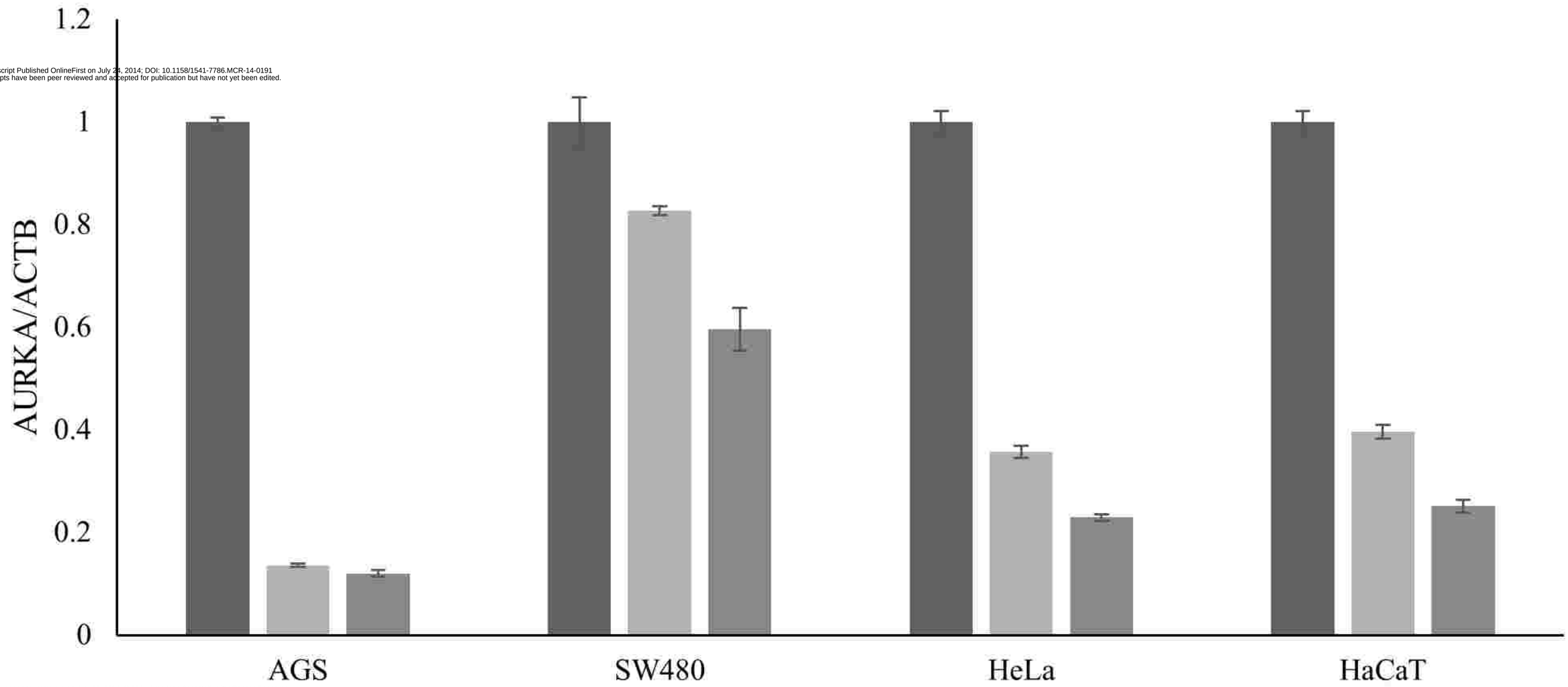

Author Manuscript Published OnlineFirst on July 24, 2014; DOI: 10.1158/1541-7786.MCR-14-0191
Author manuscripts have been peer reviewed and accepted for publication but have not yet been edited.

Fig. 2B

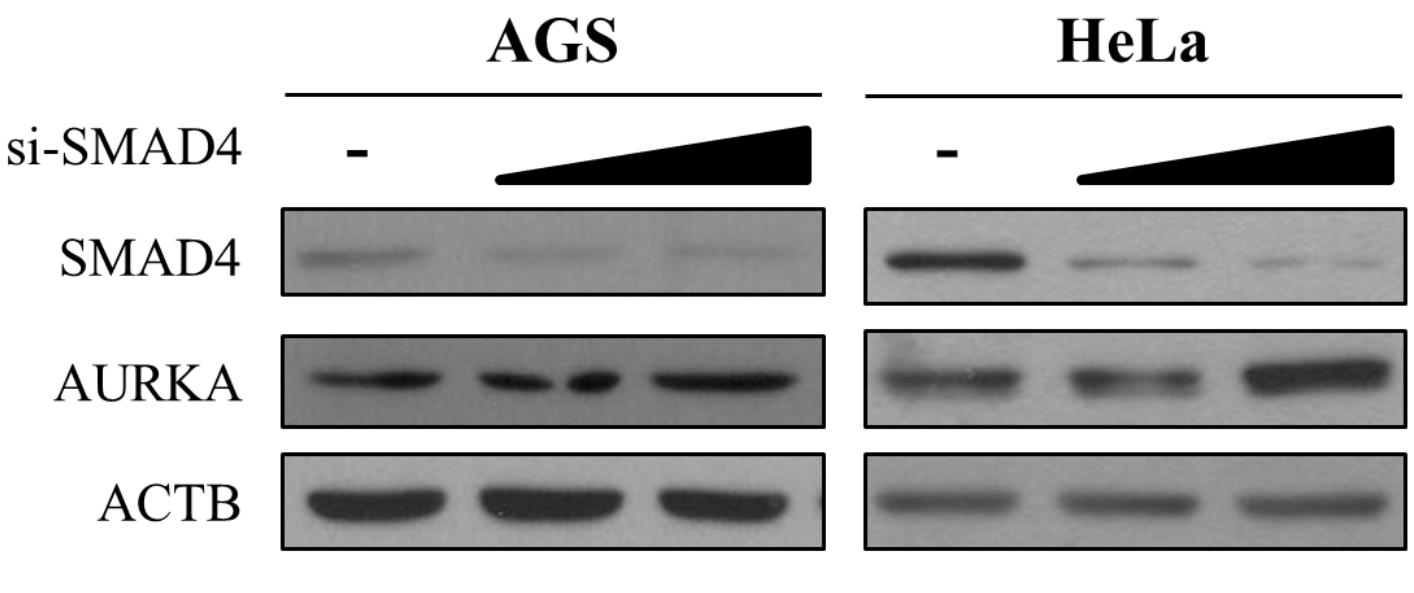

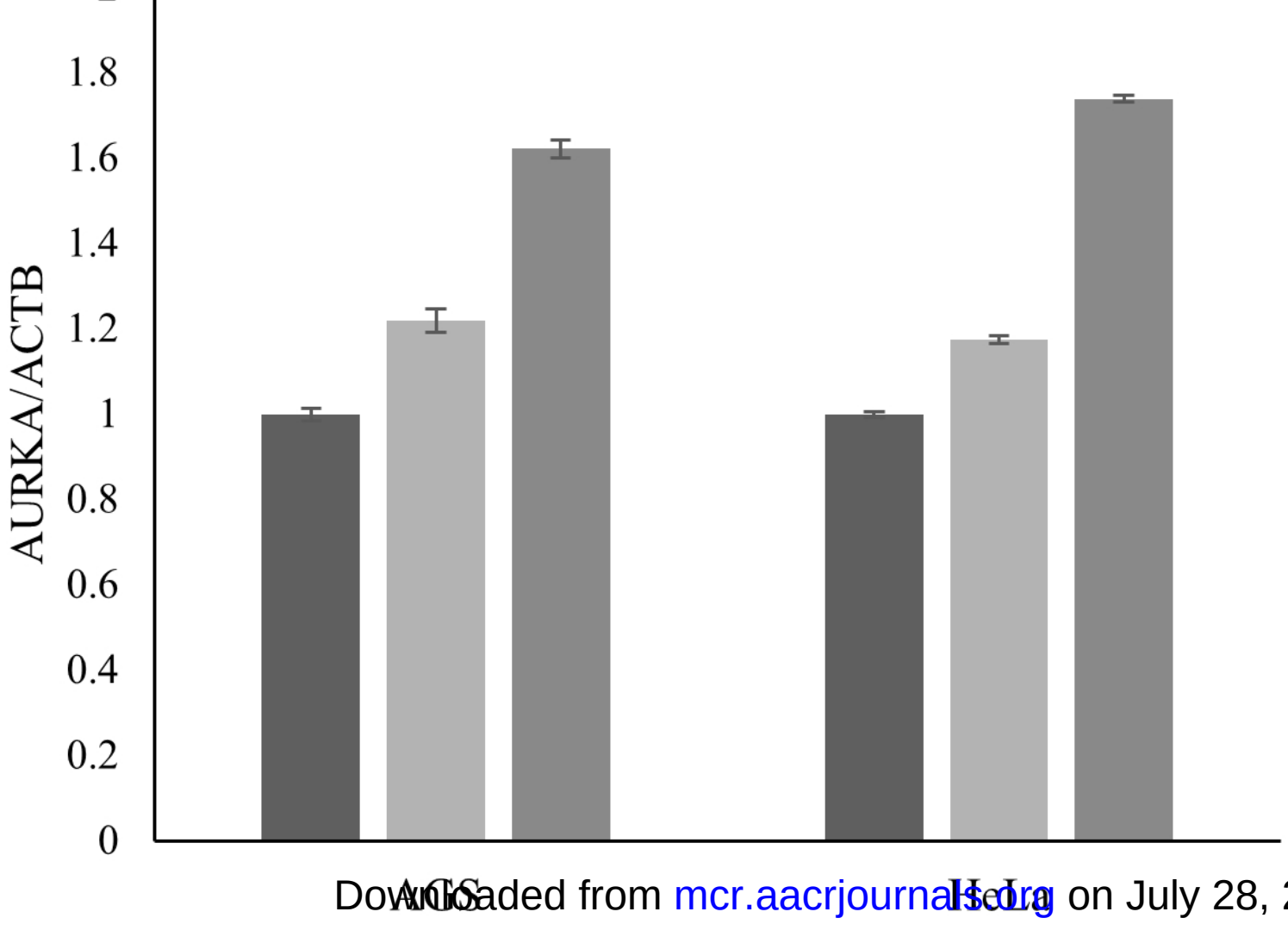

Author Manuscript Published OnlineFirst on July 24, 2014; DOI: 10.1158/1541-7786.MCR-14-0191

Fig. 2C

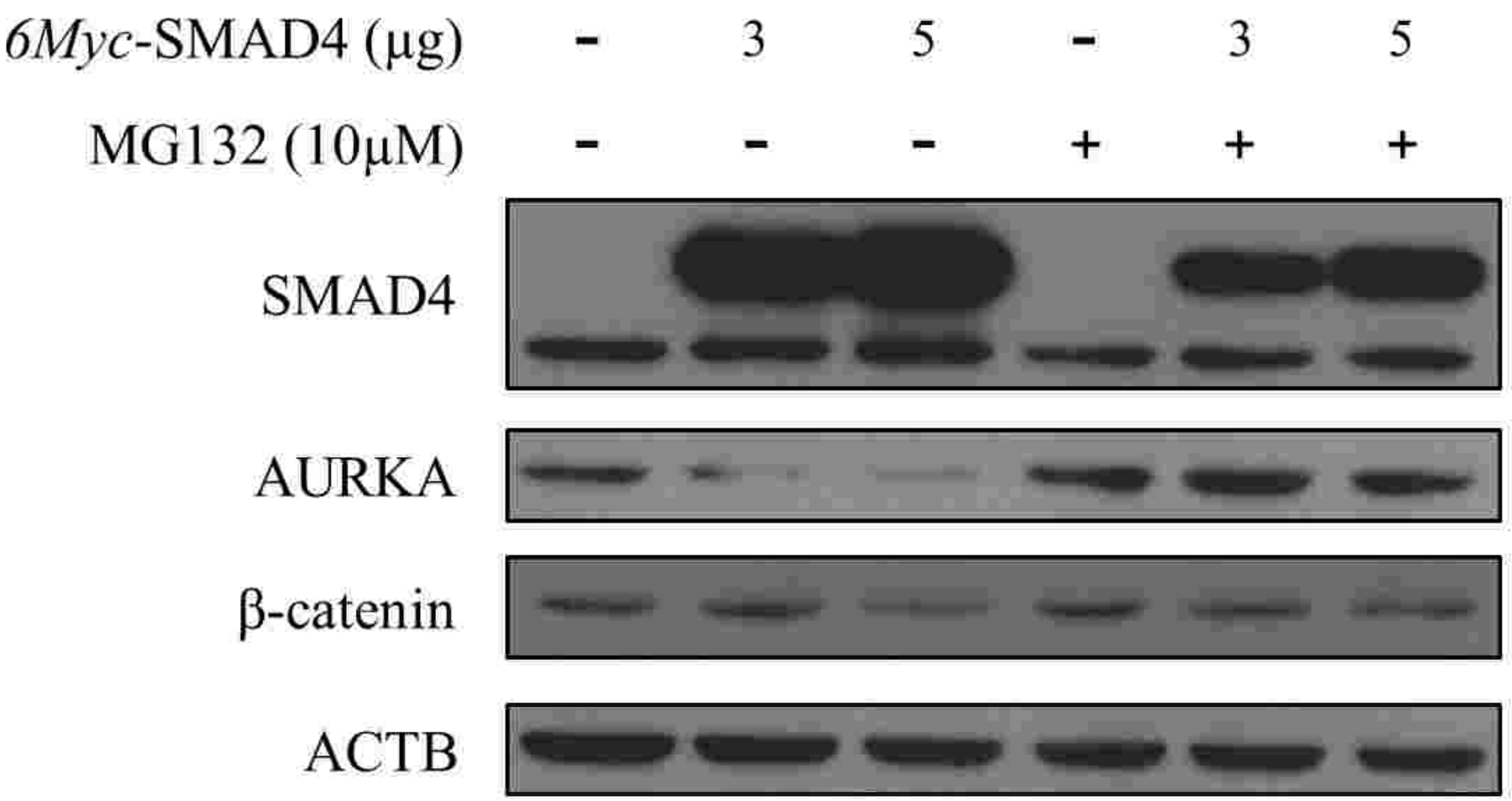

Fig. 2D

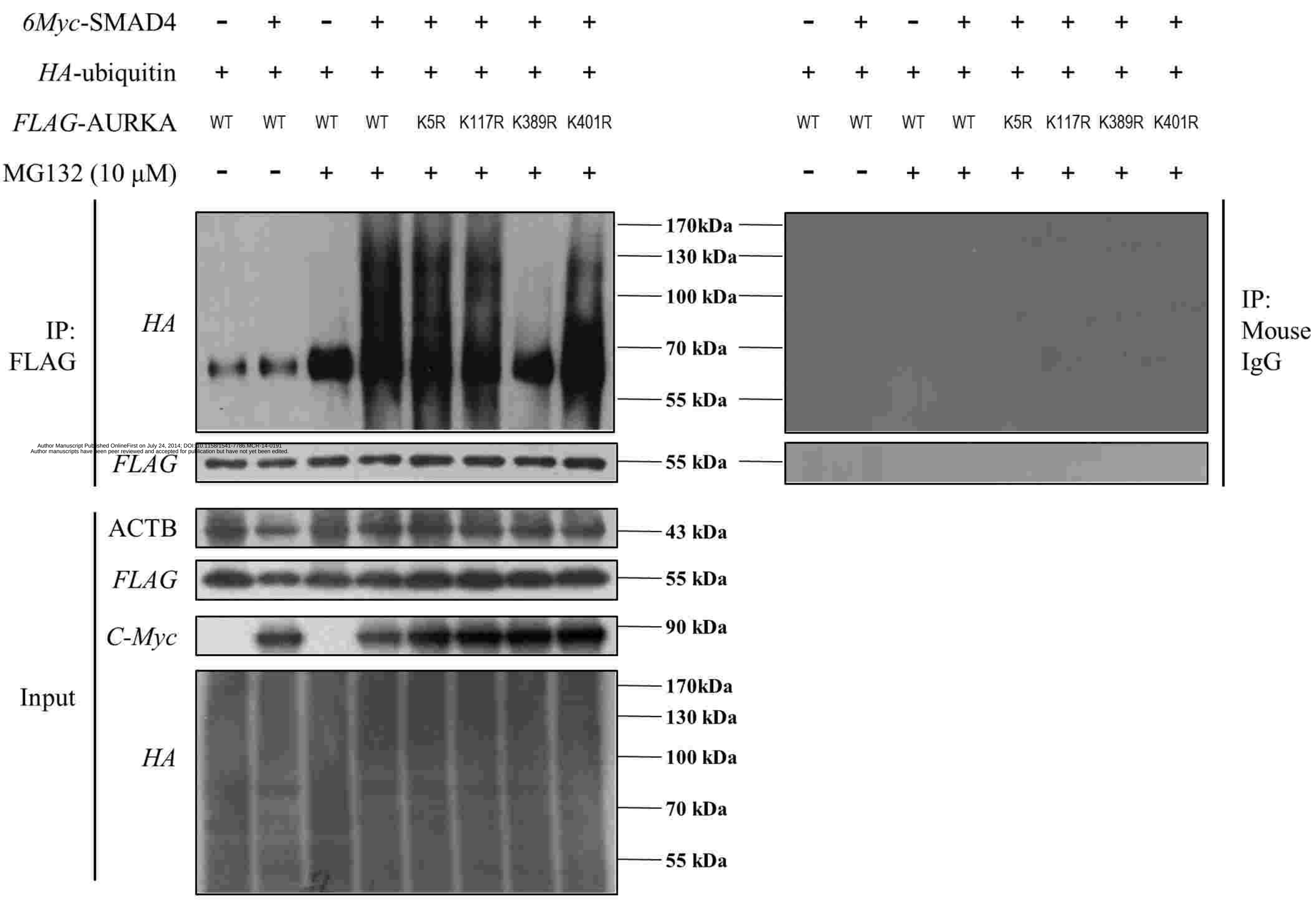

Fig. 3A

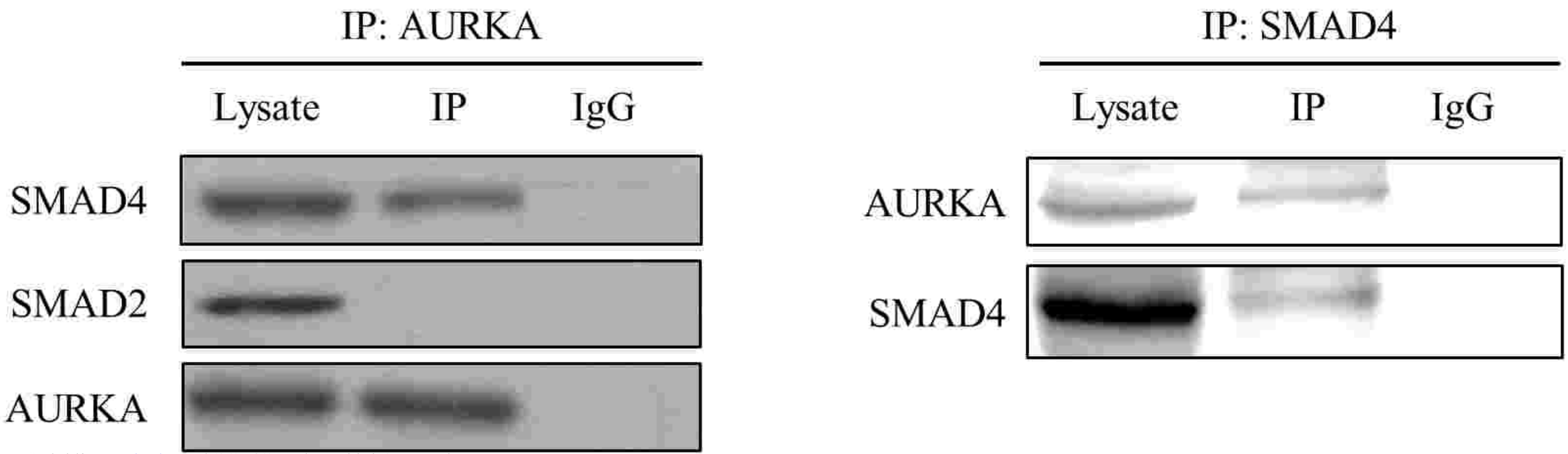

Fig. 3B

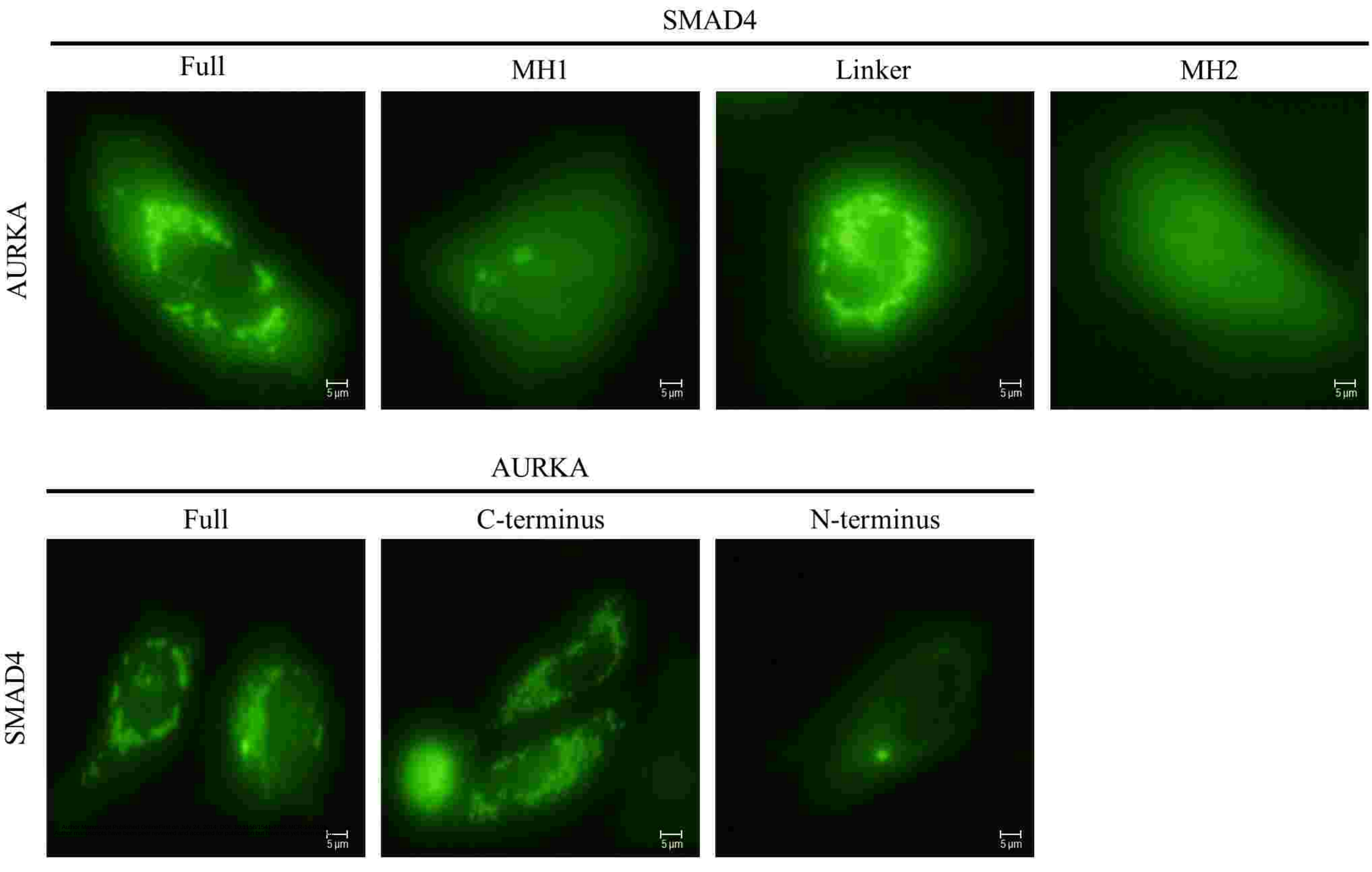

Fig. 3C

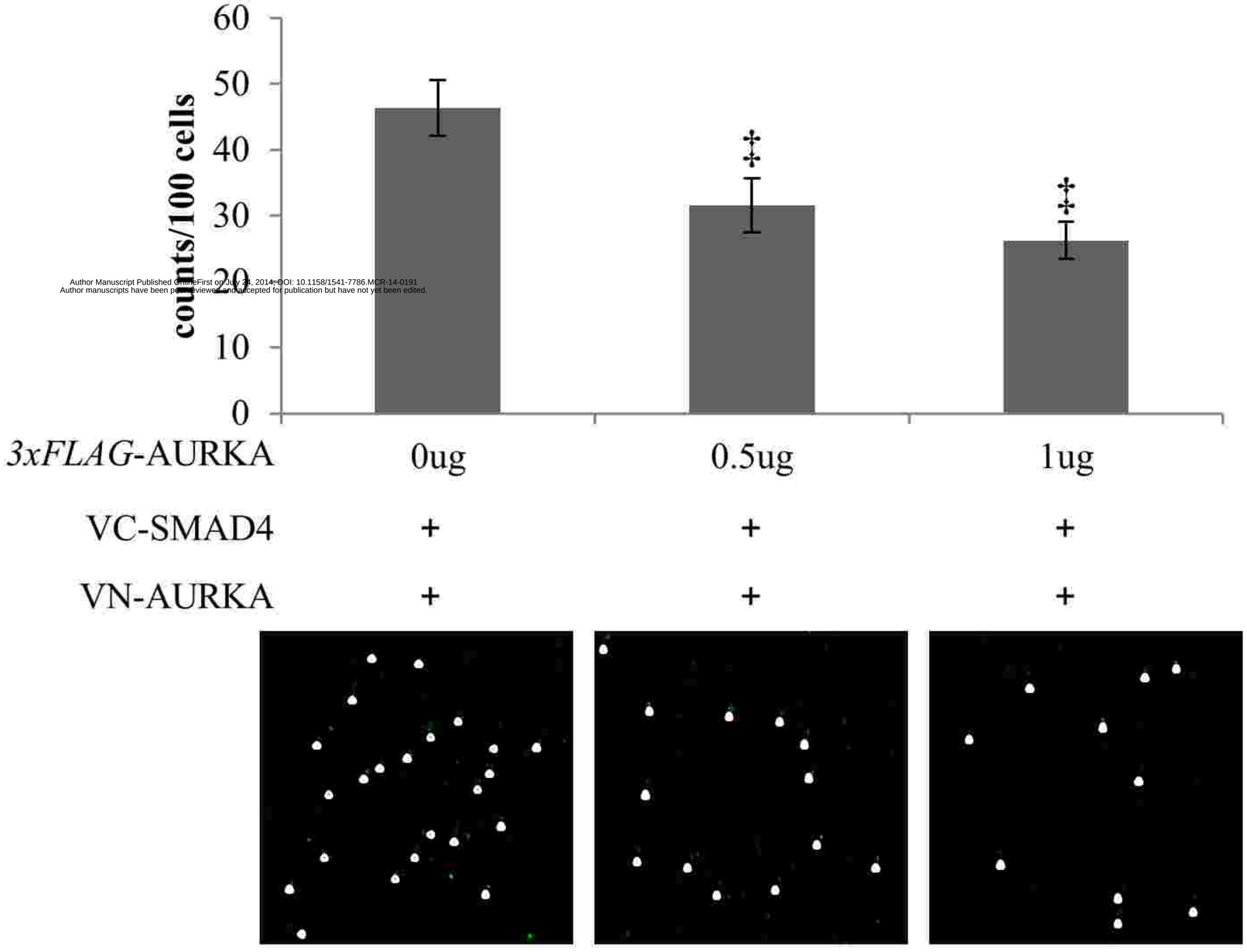

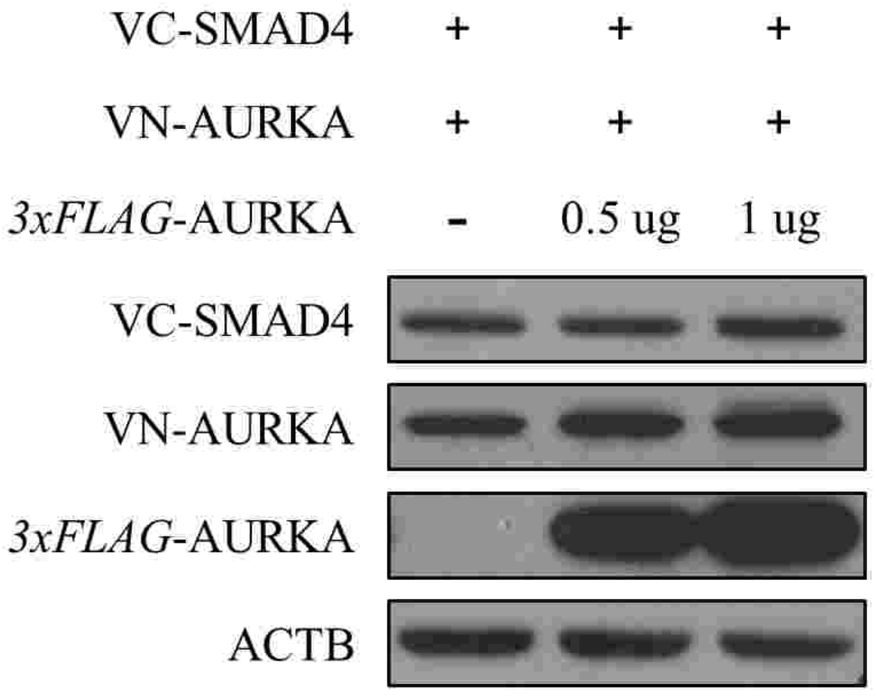

Fig. 3D

Fig. 3E

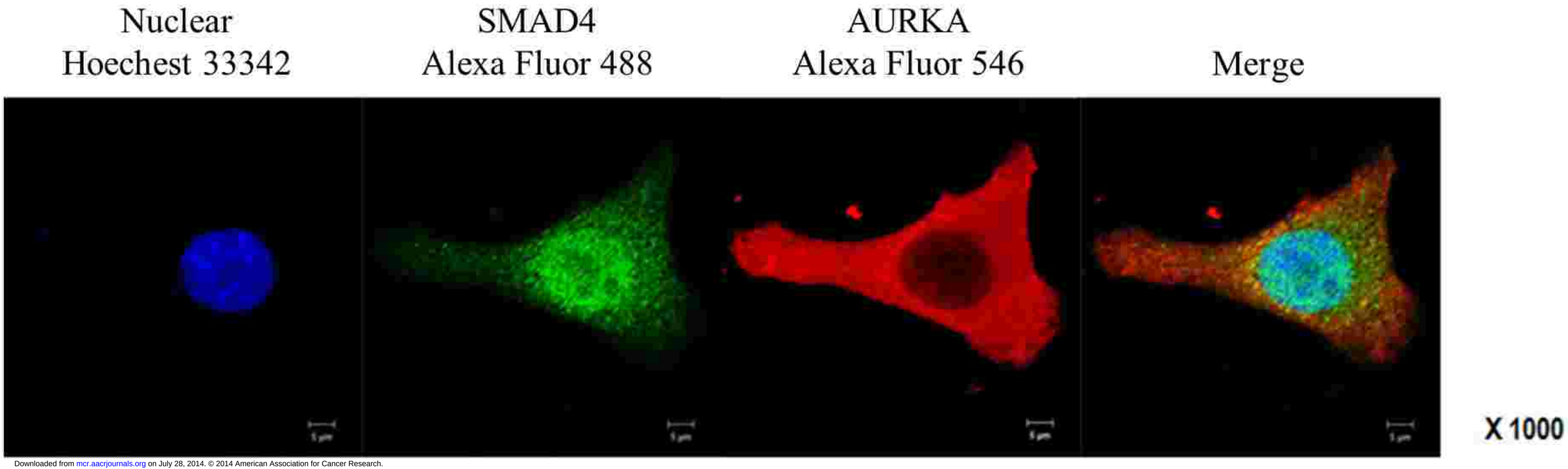

Fig. 3F

	IP: FLAG											
	Lysate				IP				IgG			
HA-SMAD4-F	+	-	-	-	+	-	-	-	+	-	-	-
HA-SMAD4-MH1	-	+	-	-	-	+	-	-	-	+	-	-
HA-SMAD4-MH2	-	-	+	-	-	-	+	-	-	-	+	-
HA-SMAD4-Linker	-	-	-	+	-	-	-	+	-	-	-	+
FLAG-AURKA	+	+	+	+	+	+	+	+	+	+	+	+

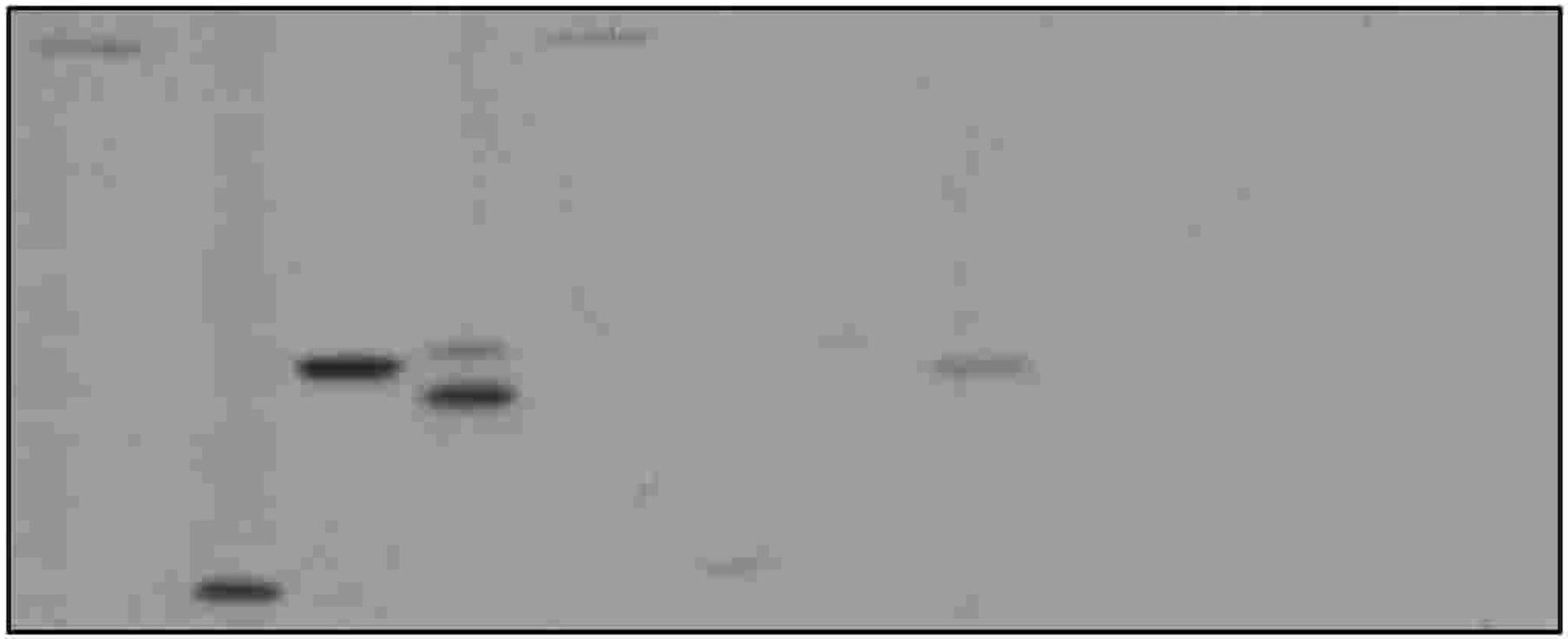

Author Manuscript Published OnlineFirst on July 24, 2014; DOI: 10.1158/1541-7786.MCR-14-0191
Author manuscripts have been peer reviewed and accepted for publication but have not yet been edited.

Fig. 3G

Author Manuscript Published OnlineFirst on July 24, 2014; DOI: 10.1158/1541-7786.MCR-14-0191
Author manuscripts have been peer reviewed and accepted for publication but have not yet been edited.

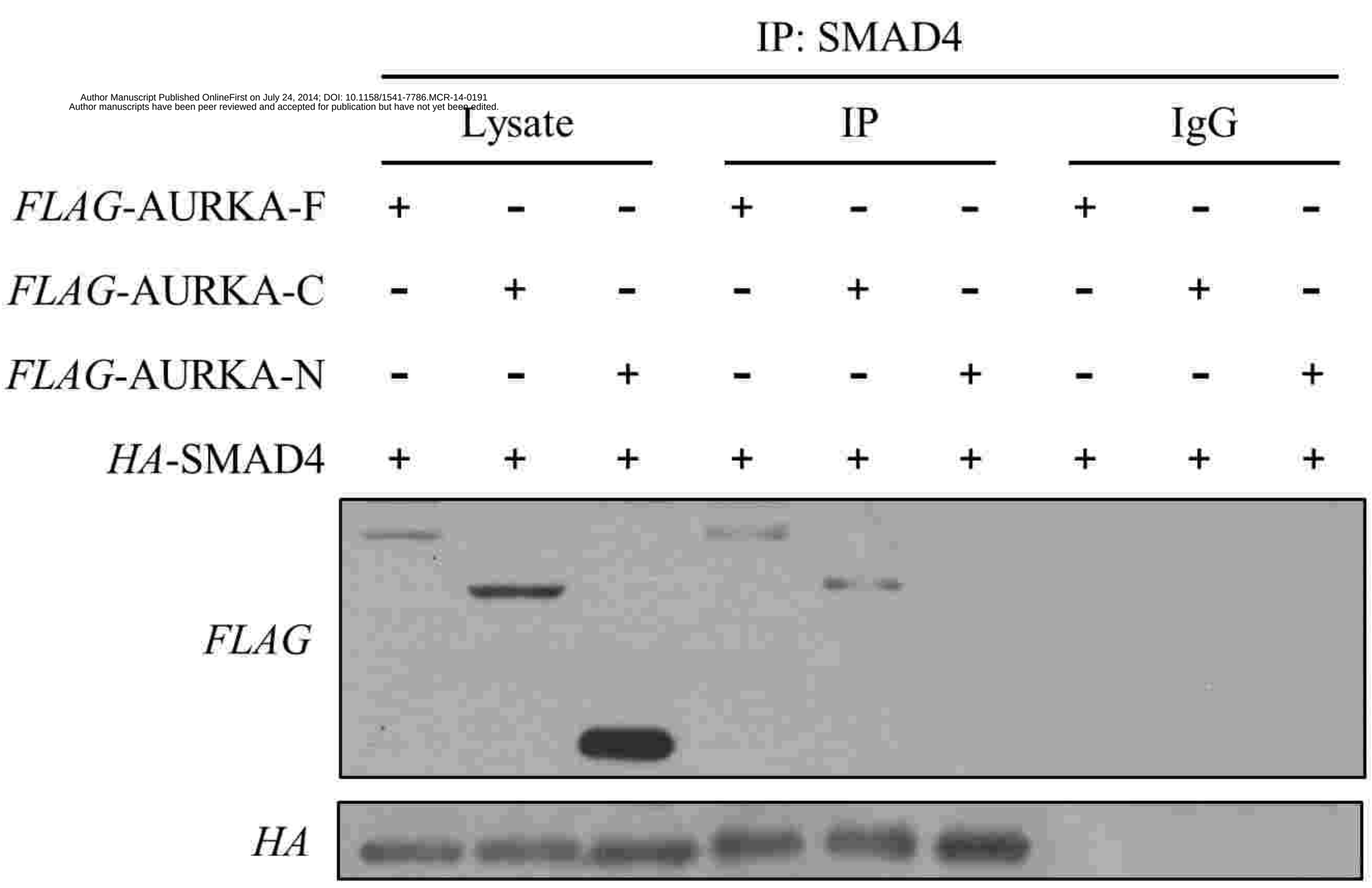

Fig. 3H

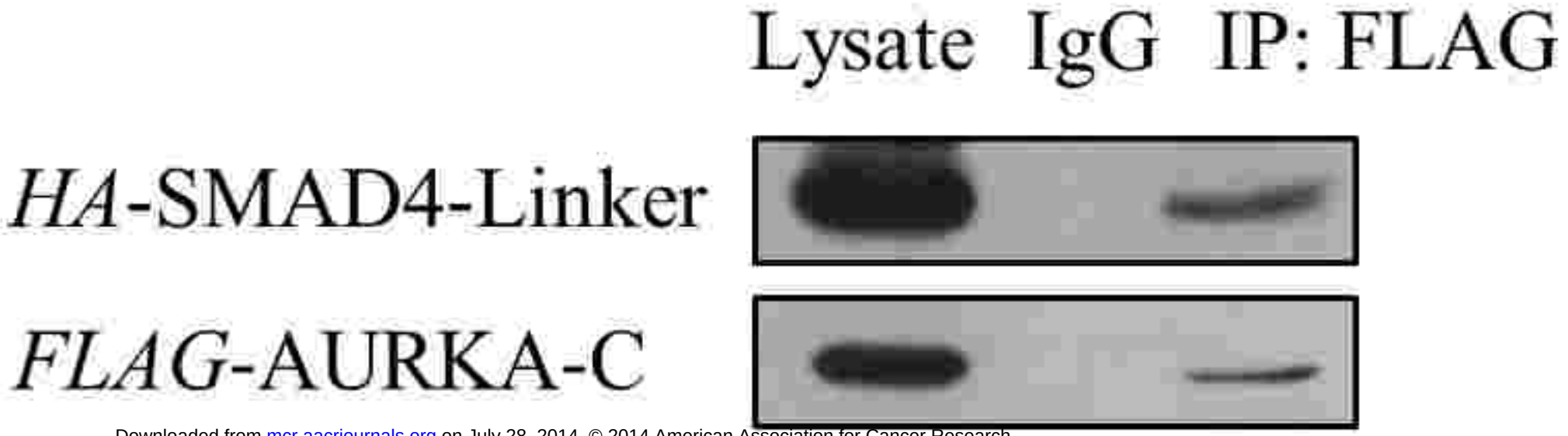

Fig. 3I

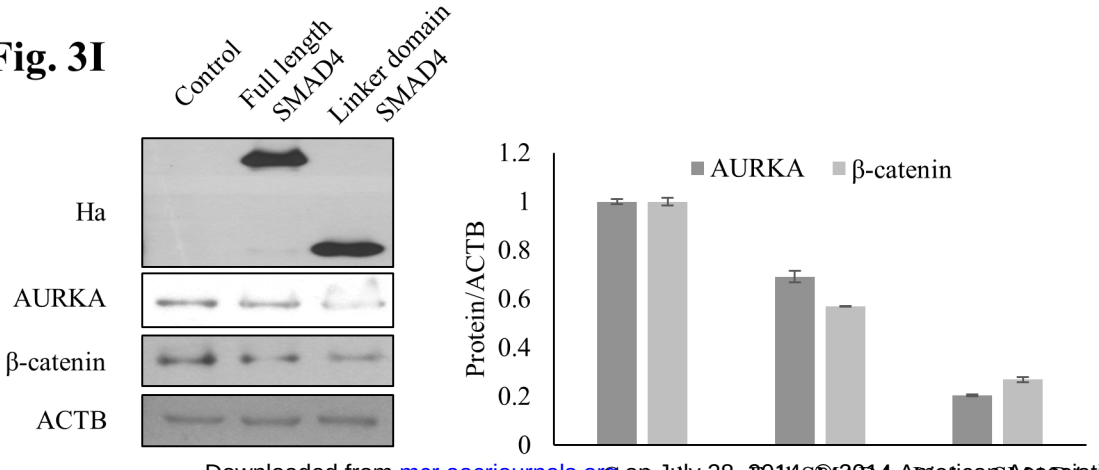

Fig. 4A

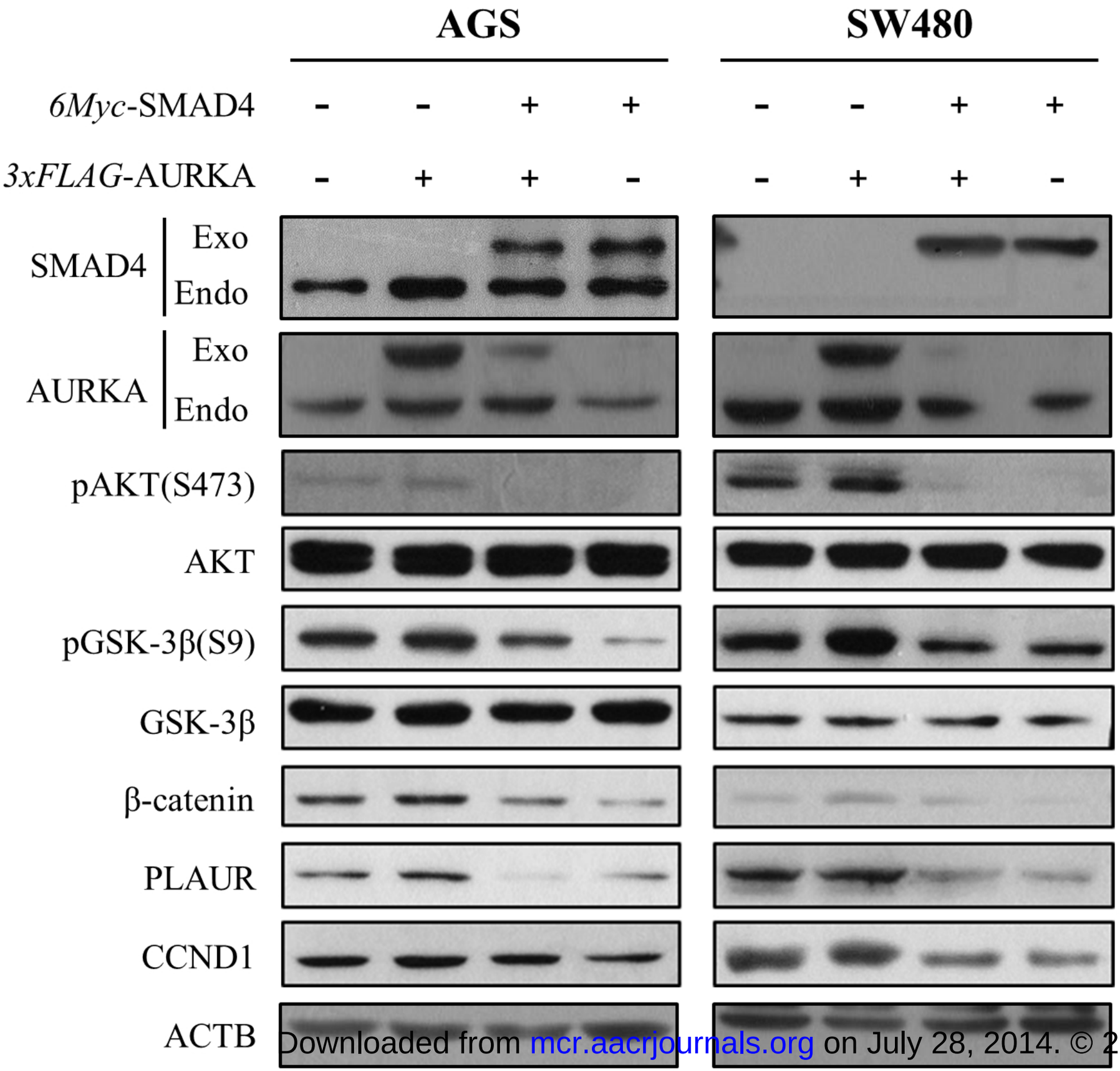

Fig. 4B

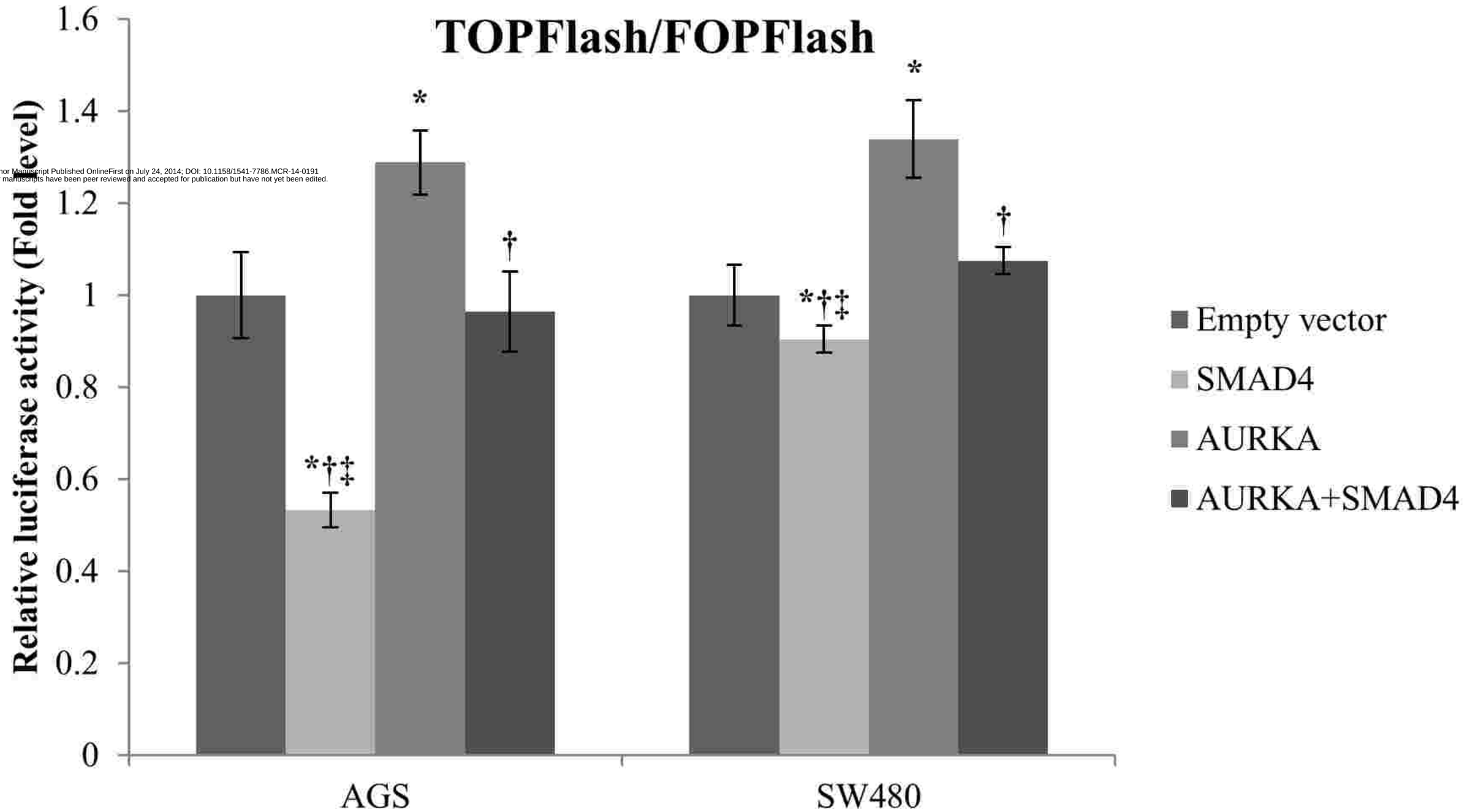

Fig. 4C

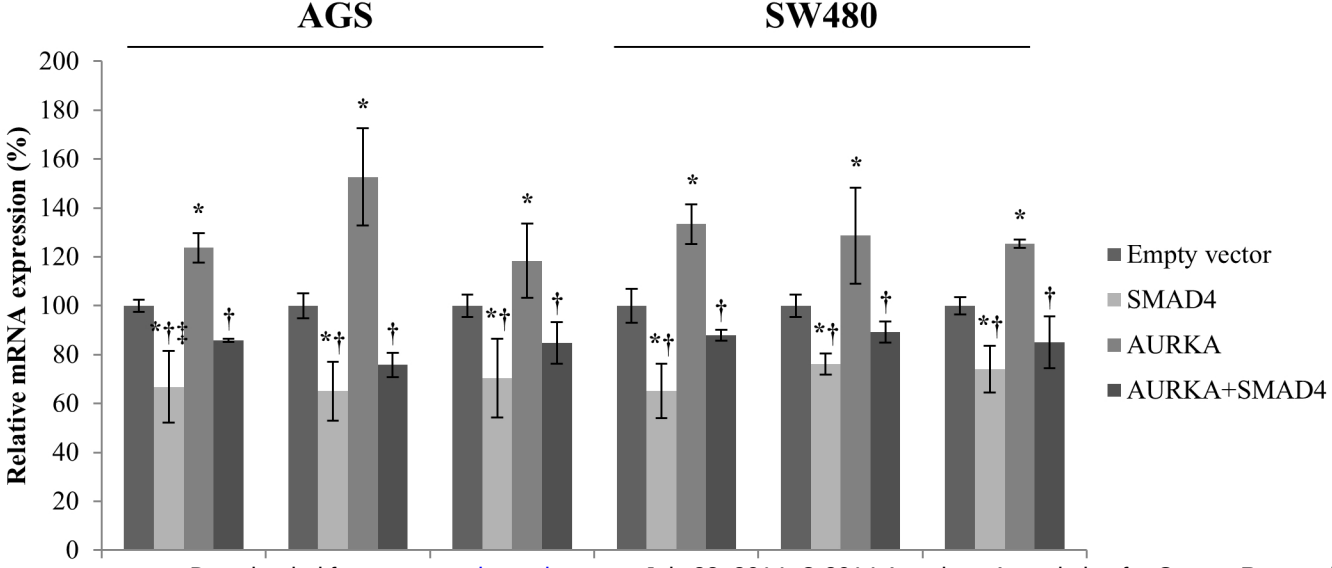

Fig. 5A

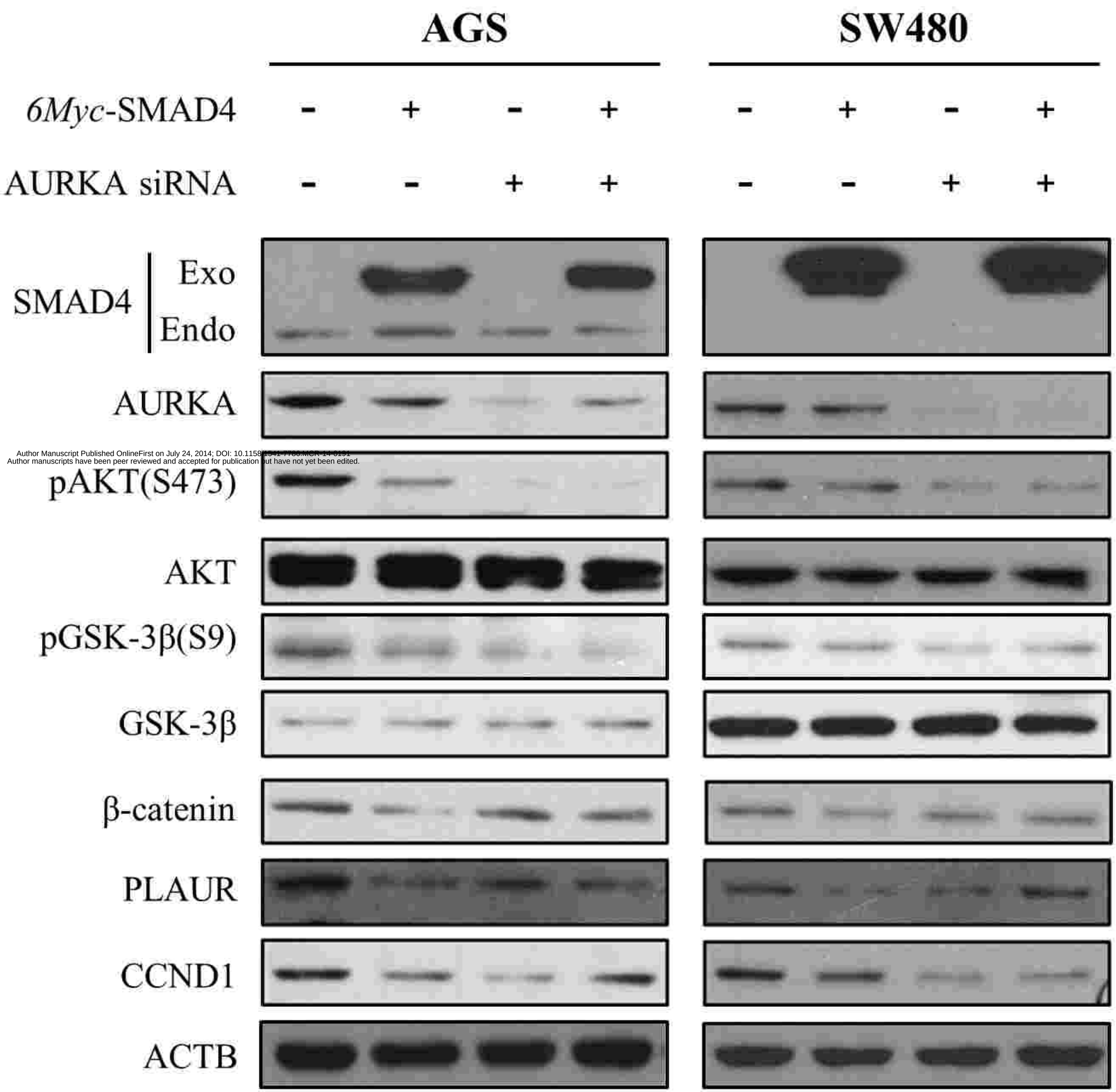

Fig. 5B

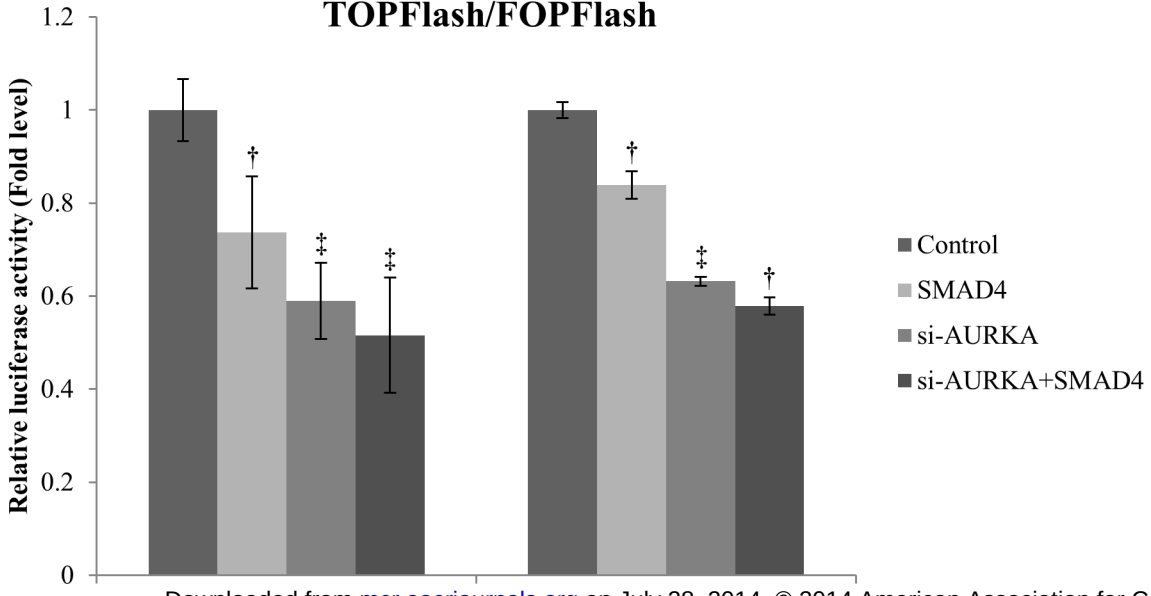

Fig. 5C

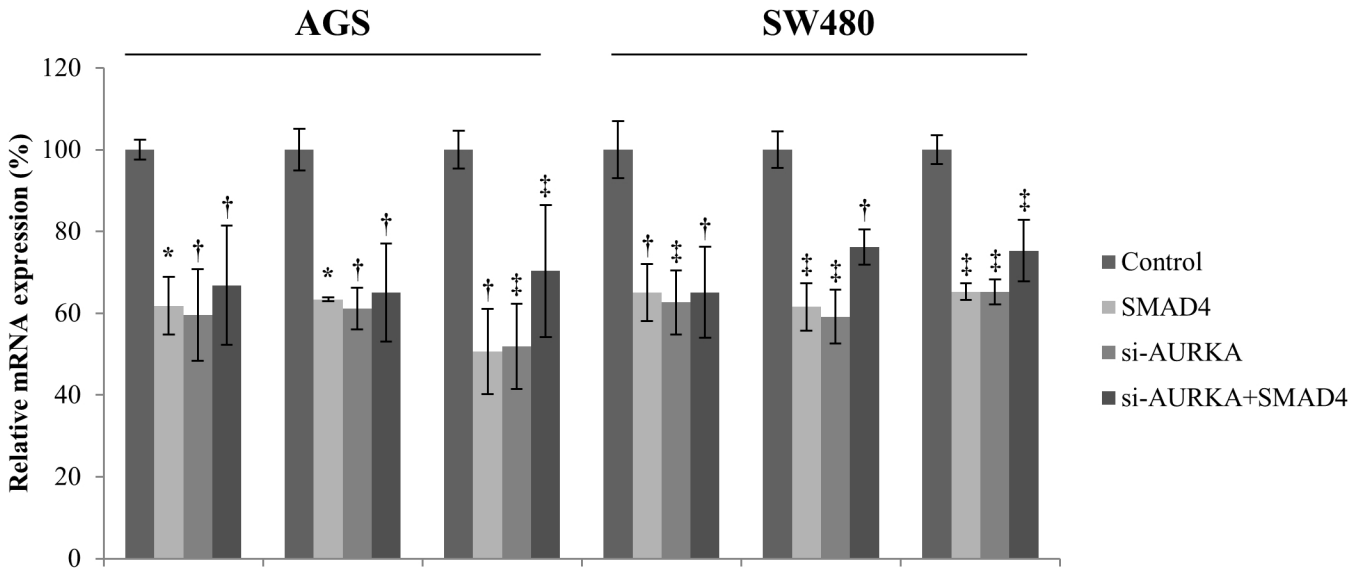

Author Manuscript Published OnlineFirst on July 24, 2014; DOI: 10.1158/1541-7786.MCR-14-0191

Fig. 6A

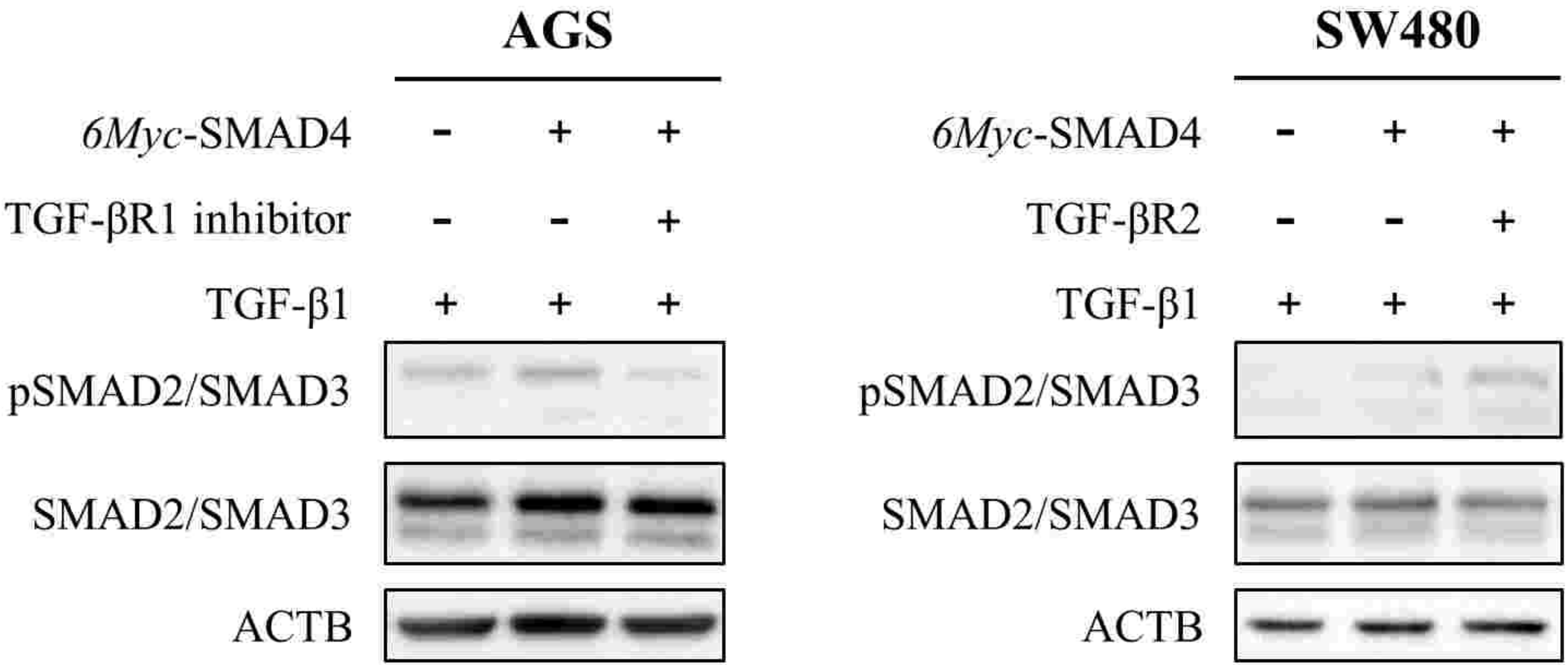

Fig. 6B

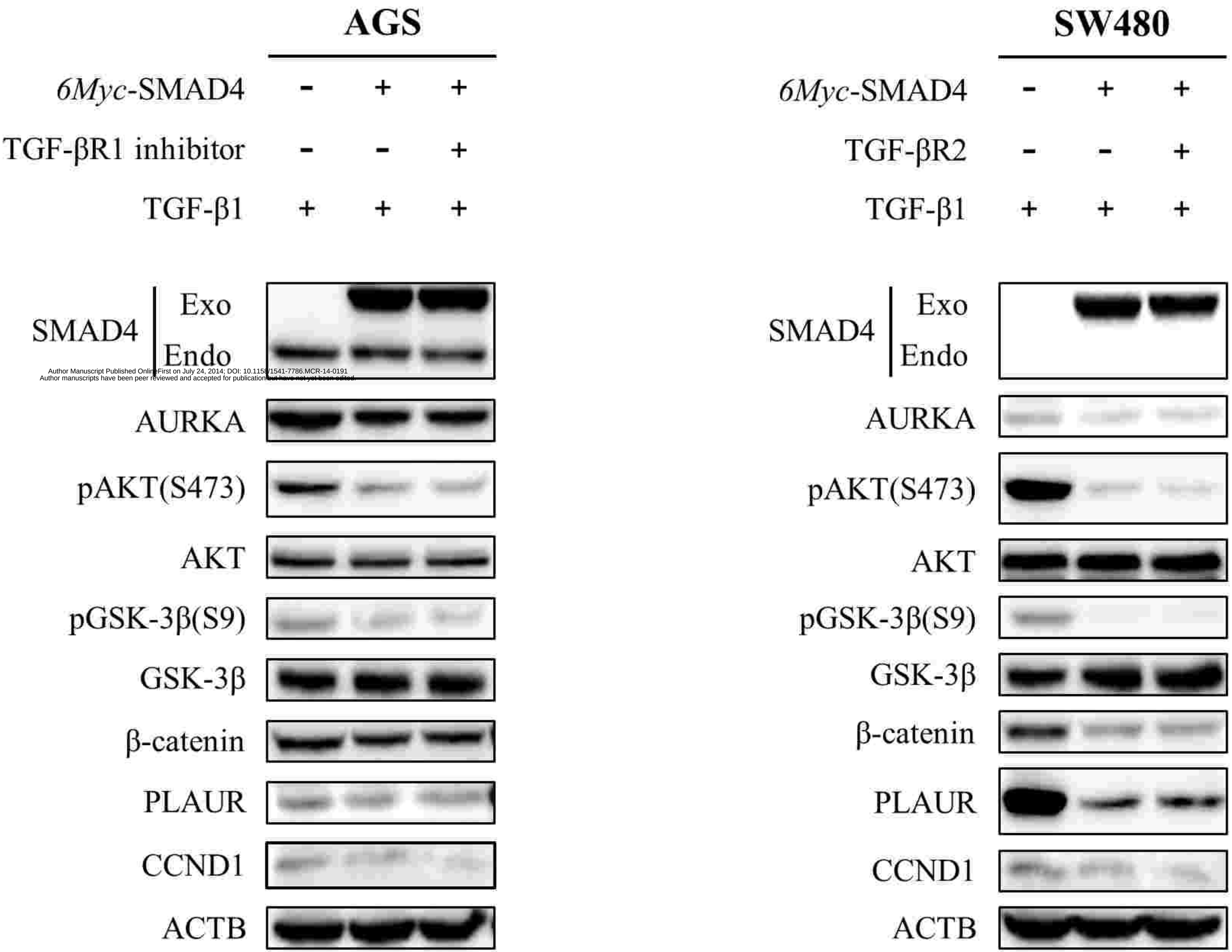

Figure 7A

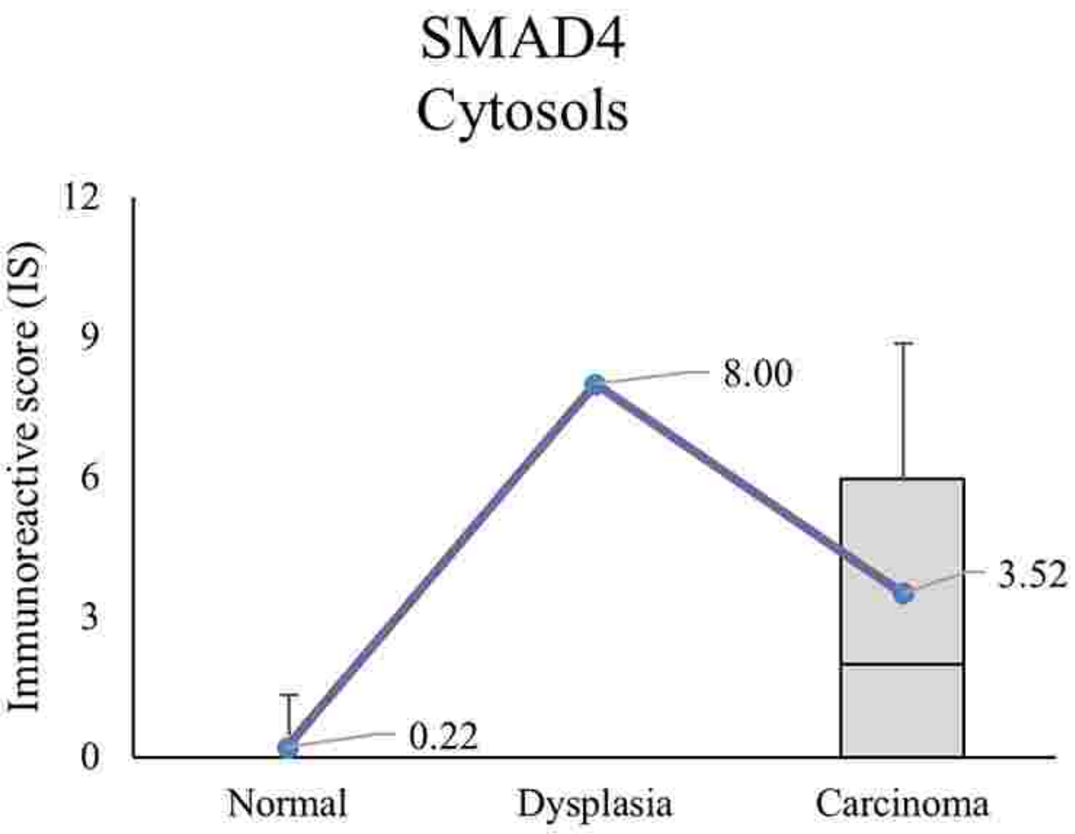

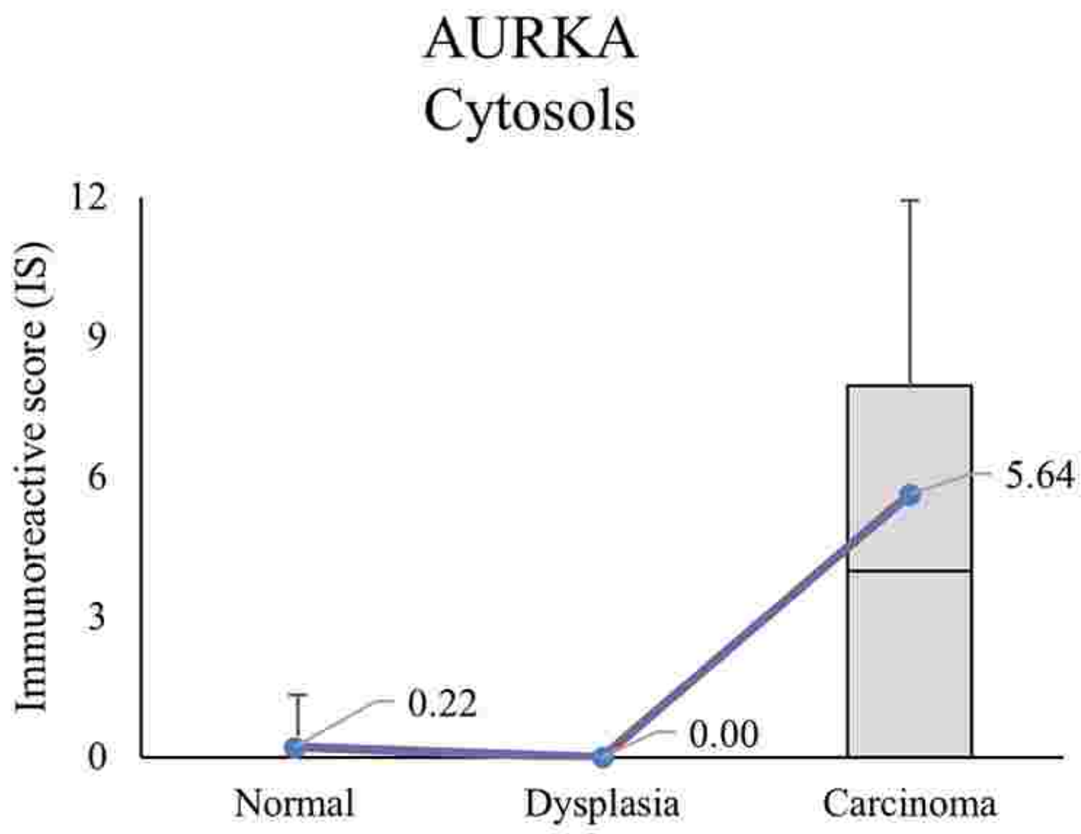

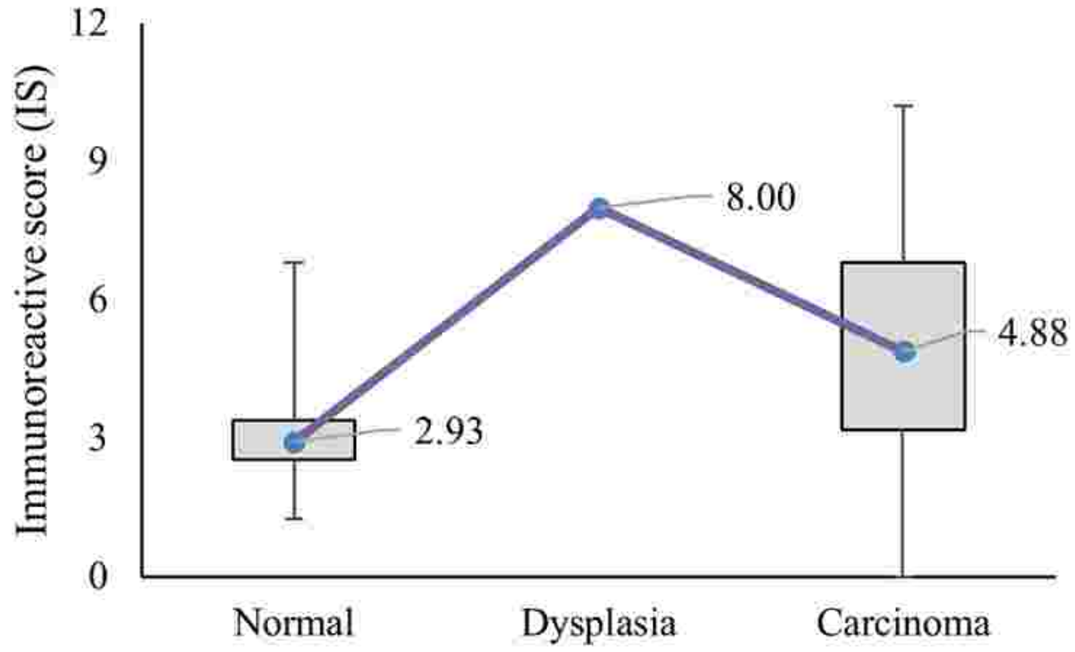

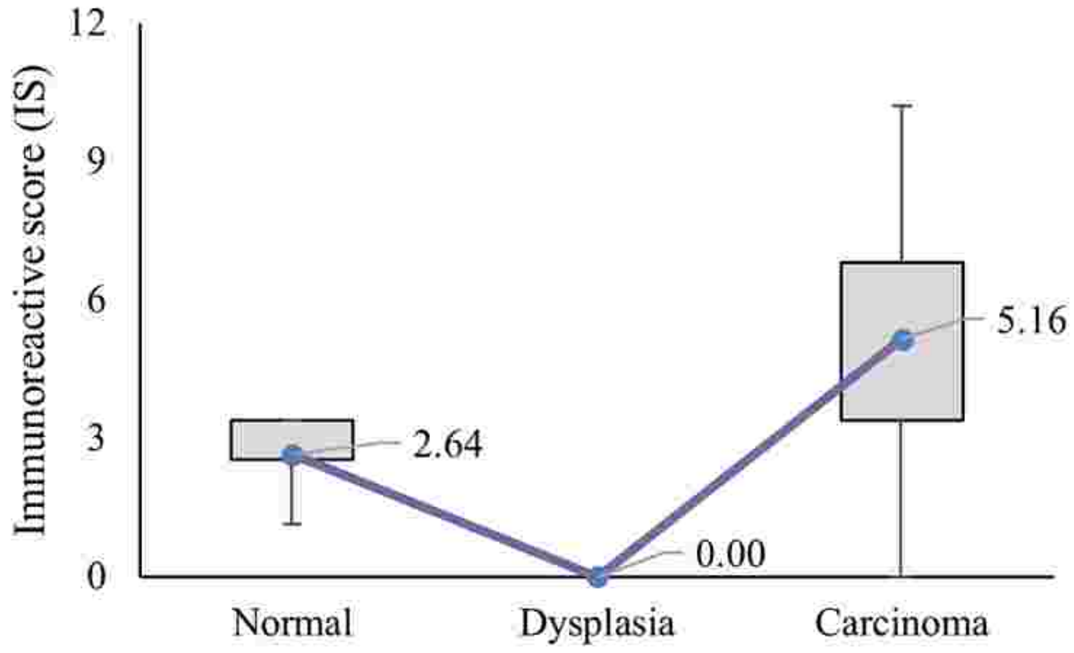

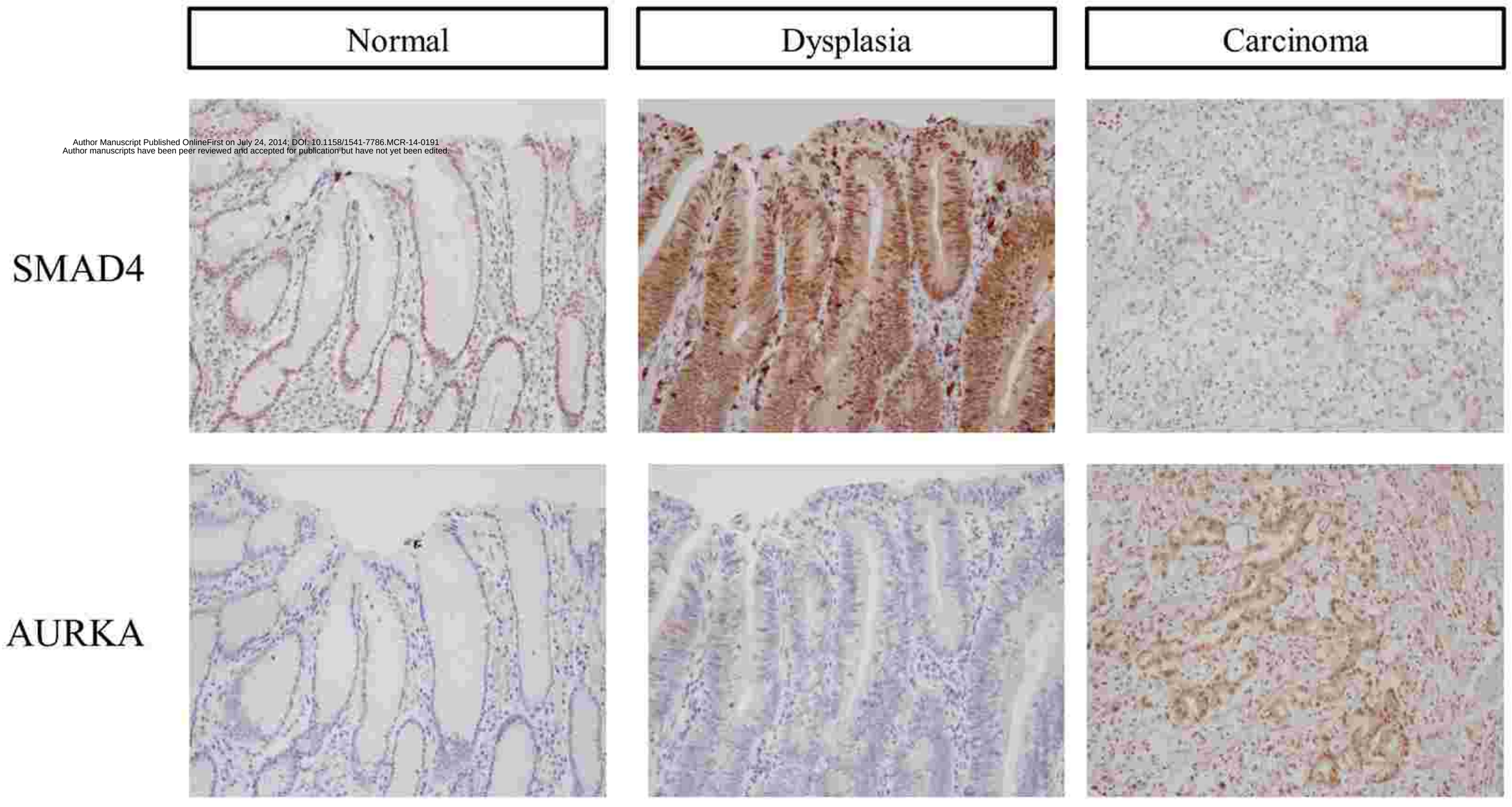

Figure 7B

Author Manuscript Published OnlineFirst on July 24, 2014; DOI: 10.1158/1541-7786.MCR-14-0191
Author manuscripts have been peer reviewed and accepted for publication but have not yet been edited.

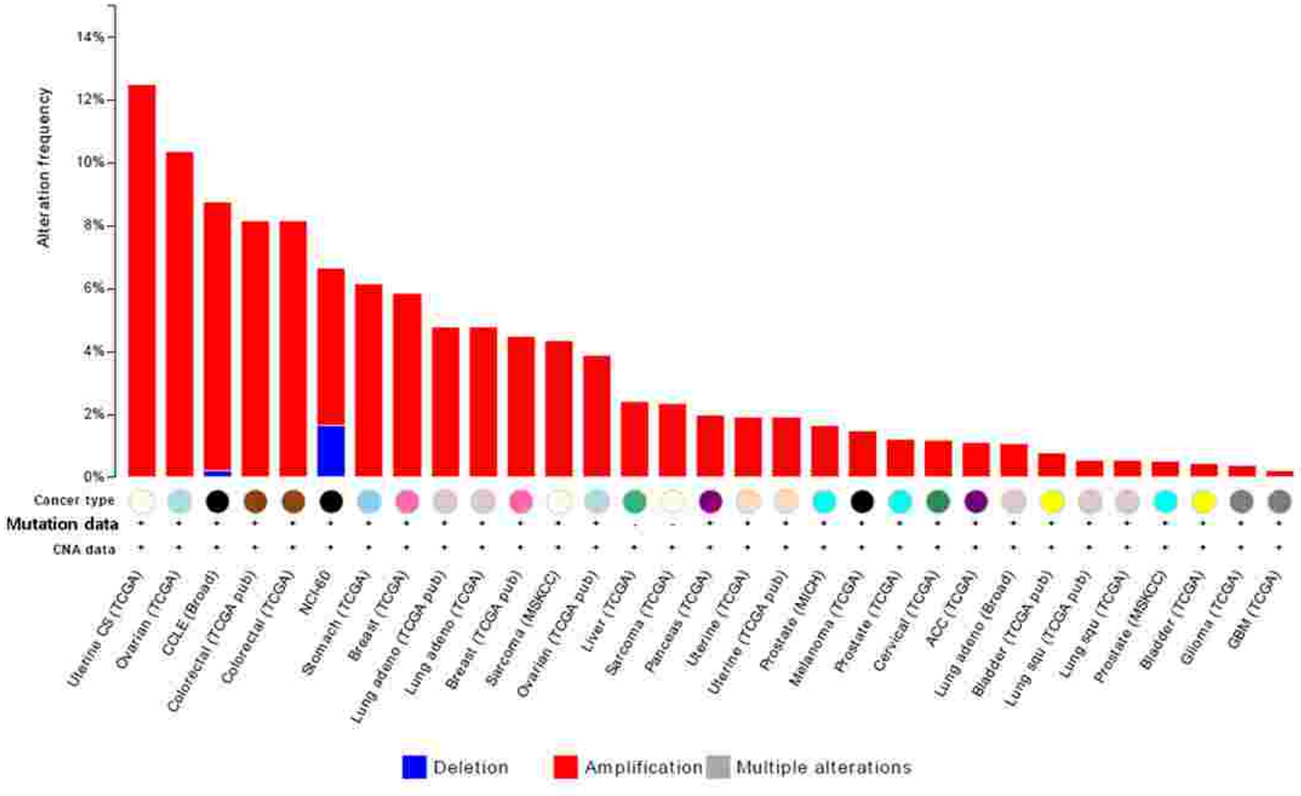

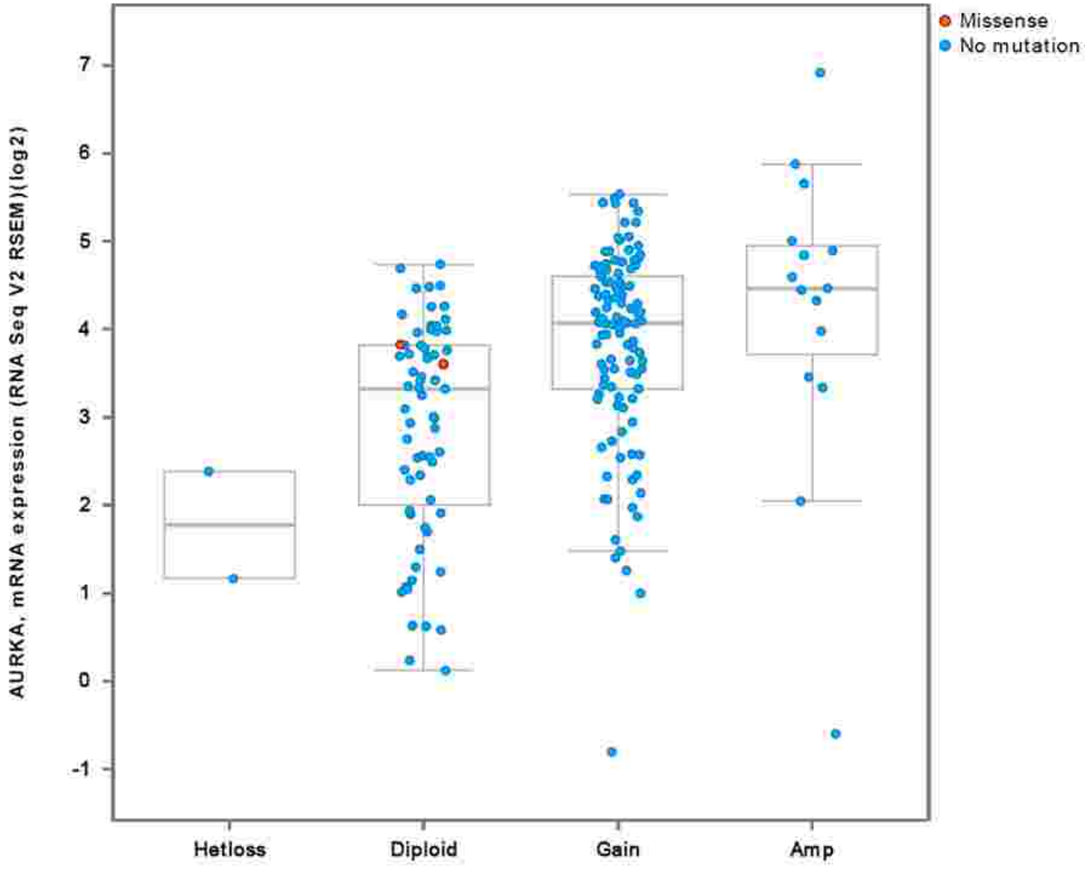

Figure 7C

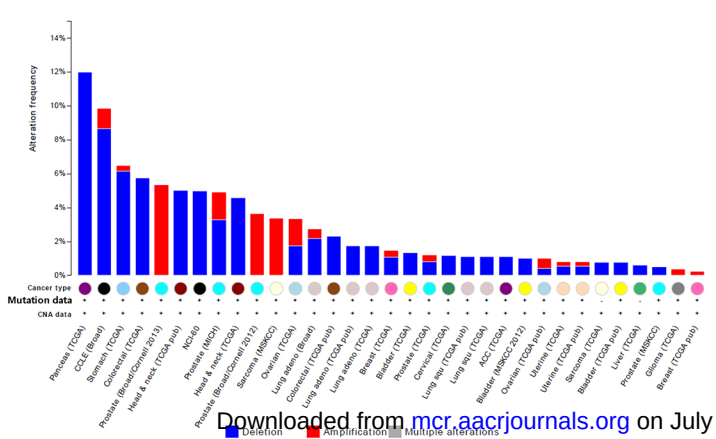

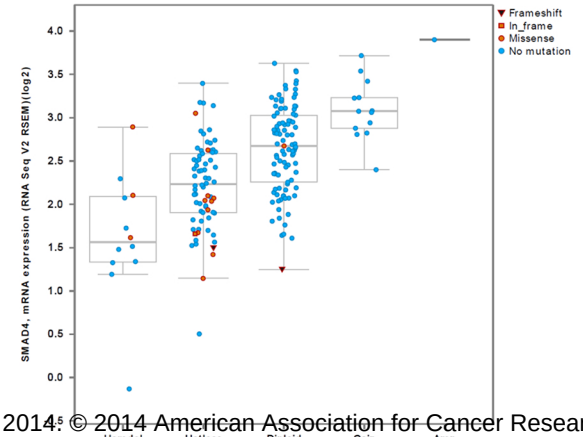

Figure 7D

Author Manuscript Published OnlineFirst on July 24, 2014; DOI: 10.1158/1541-7786.MCR-14-0191

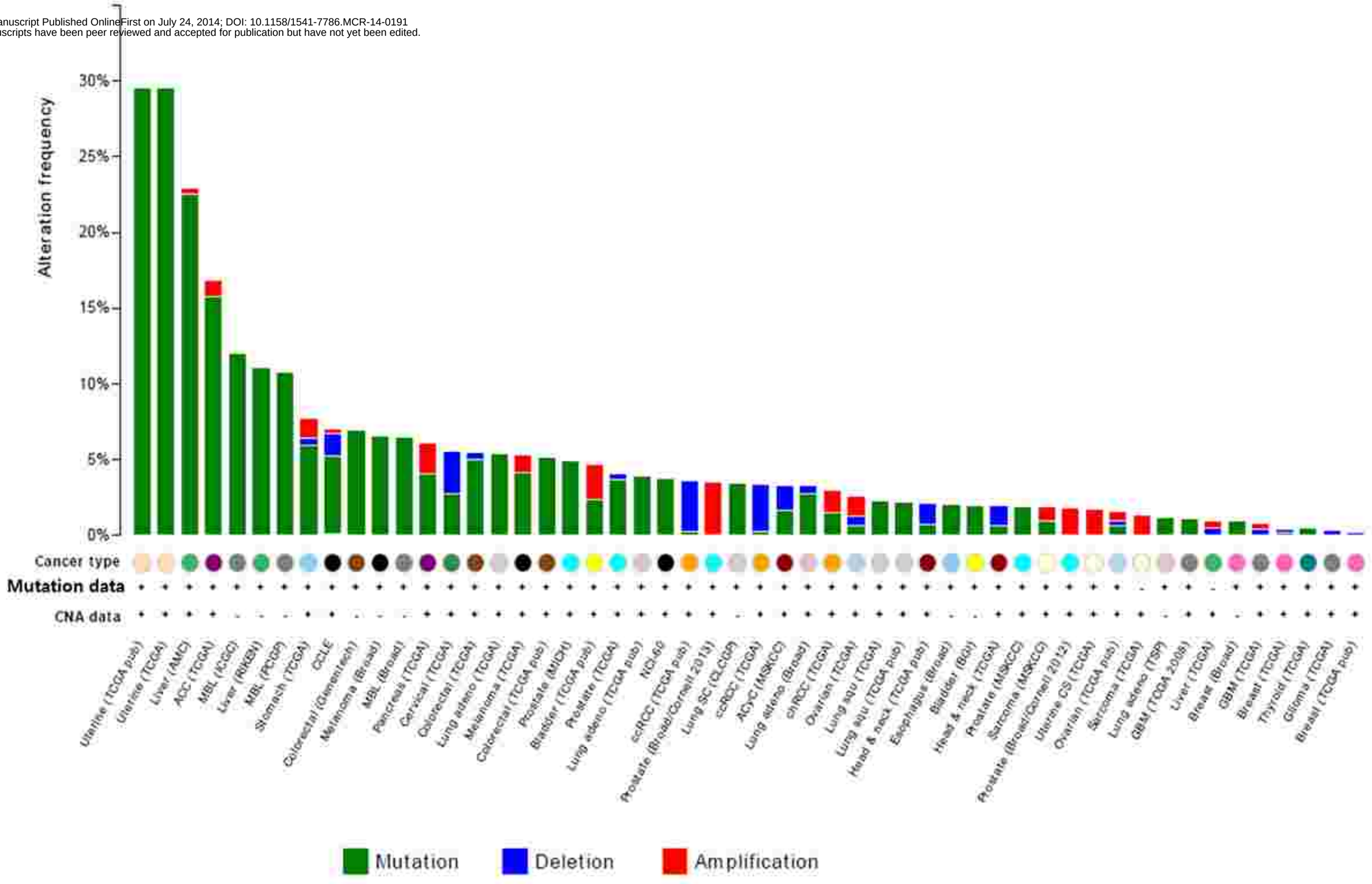

Fig. 7E